Geoderma 429 (2023) 116253

Contents lists available at ScienceDirect

Geoderma

journal homepage: www.elsevier.com/locate/geoderma

Plant available water predicted by a flux-based approach

Marina Luciana Abreu de Melo [a,*], Leonardo Inforsato [a], Everton Alves Rodrigues Pinheiro [b], Quirijn de Jong van Lier [a]

[a] Soil Physics Laboratory, Center for Nuclear Energy in Agriculture, University of São Paulo, P.O. Box 96, Piracicaba, São Paulo, Brazil
[b] Federal University of Tocantins, Gurupi, Tocantins 77402-970, Brazil

ARTICLE INFO

Keywords:
Field capacity
Wilting point
Limiting point
Flux-criterion
Matric flux potential
Residual transpiration

ABSTRACT

Plant available water (PAW) is an important indicator of soil suitability for crop growth and biomass production. Total available water (TAW) is defined as the difference between the water content at field capacity (FC) and at wilting point (WP). The readily available water (RAW) is a fraction of TAW defined as the water content between FC and the limiting point (LP). The challenge in determining TAW and RAW lies in the correct determination of FC, WP, and LP. We propose a process-based approach to address the issue, referenced as flux-based method (FBM). Five scenarios were used to assess the FBM: (1) generic soil-plant-atmosphere conditions, from which sensitivity analyses were performed; (2) a maize crop on several soils to compare the predictions of the FBM and the traditional FAO method; (3) mean plant-atmosphere conditions to map PAW from soil texture using the FBM and the FAO method; (4) a field experiment with a fully irrigated soybean crop; and (5) a field experiment with a common bean crop under water deficit. Resulting flux-based TAW and RAW showed high sensitivity to root length density and soil hydraulic parameters. The FBM tended to predict higher water contents at FC than the FAO method for maize crop scenarios. Texture triangles to predict TAW and RAW showed that the differences between the predictions of FBM and FAO are mostly due to the distinct values for FC, and for the LP, respectively. For both observed scenarios of soybean and common bean crops, the predictions of the FBM were plausible with time series of observed data. The FBM allows predicting PAW in Van Genuchten – Mualem type soils for different FC flux criteria, soil depths, root densities, and dynamic potential transpiration rates.

1. Introduction

Soil water mediates important ecosystem services in the critical zone at local, regional, and global scales, including functions related to biomass production of natural and agricultural ecosystems, which are partially regulated by root water uptake (de Jong van Lier et al., 2022; Skaggs et al., 2006). Not all soil water is available to plants, and plant available water (PAW) can be expressed as a fraction of total soil water storage (Bhattacharya, 2019; Ferreira, 2017; Kirkham, 2005; Silva et al., 2014). The PAW fraction, also referred to as total available water (TAW), is commonly defined as the difference between the volume-based water content at field capacity (FC) and at permanent wilting point (WP). Another term with a similar meaning, but with a slightly different purpose, is the readily available water (RAW). The lower limit of RAW is the limiting soil water content (LP), which is related to the limiting soil hydraulic conditions and indicates the onset of plant drought stress (Metselaar and de Jong van Lier, 2007). Here, the term PAW will be used to encompass both TAW and RAW fractions.

Whereas the value of PAW is important for many applications, e.g. for irrigation scheduling and hydrological modeling, its field determination is hardly ever performed. Ideally, PAW should be determined considering the specific combination of plant, soil, and weather conditions. Due to its dependence on the interactions between the plant, the soil, and the atmospheric conditions, procedures for more accurate determination of PAW are cumbersome and labor-intensive, requiring an extensive number of measurements under controlled conditions (de Jong van Lier et al., 2022). Soil texture, structure, fertility, along with crop type, root characteristics, plant age, crop drought tolerance, as well as climatic conditions are just some of the many factors that can influence PAW (Liu et al., 2022; Luz et al., 2022; Pinheiro et al., 2018).

A standard method to quantify PAW was proposed by the Food and Agriculture Organization (FAO) in Irrigation and Drainage Paper No. 56 (Allen et al., 1998), here referred to as the FAO method. As the water held in the soil above FC is destined to drain in a few days, and the water

* Corresponding author.
E-mail address: melo.marina@usp.br (M.L.A. de Melo).

https://doi.org/10.1016/j.geoderma.2022.116253
Received 25 April 2022; Received in revised form 24 October 2022; Accepted 1 November 2022
Available online 11 November 2022

held below WP cannot be extracted by plant roots, according to this method the total available water (TAW, $m^3\ m^{-3}$) is the difference between the water content at FC and at WP. To express TAW in units of water storage (m, mm), this difference is multiplied by the effective rooting depth (Allen et al., 1998).

Although FC depends on soil layering and a criterion to define negligible flux, the soil water content at some pressure head usually between –1 m (pF 2.0) and –3.3 m (pF 2.5 or $^1/_3$ bar) is often considered as FC (de Jong van Lier and Wendroth, 2016; Logsdon, 2019). Similarly, although WP may vary according to crop type, plant age and root distribution, it is generally accepted that the soil water content at a pressure head of –150 m (pF 4.2) is a representative value for WP (Kristensen et al., 2019; Liu et al., 2022; Minasny and McBratney, 2018; Raes et al., 2018; Savage et al., 1996).

In an "adequately" wet soil, water supply to roots matches the atmospheric demand of the crop, and water uptake equals potential transpiration. When the soil water content drops below a threshold value (the limiting point, LP), soil water can no longer move towards the roots quickly enough to match the transpiration demand and the crop experiences stress (Allen et al., 1998; de Jong van Lier et al., 2013; Metselaar and de Jong van Lier, 2007). Following the FAO method, the fraction of TAW that a crop can extract from the root zone without suffering water stress is the readily available water (RAW), obtained by multiplying TAW by the depletion fraction (p). Values of parameter p are given in Allen et al. (1998) as a function of the evaporative demand of the atmosphere and of the crop sensitivity to drought stress. In practice, a value of 0.50 for p is commonly used for many crops (Allen et al., 1998).

The volume-based water contents at FC, LP, and WP allow simplifying the determination of PAW. FC is primarily a function of soil properties, whereas LP and WP depend on soil, plant, and meteorological boundary factors (de Jong Van Lier et al., 2006; Pinheiro et al., 2018; Tolk, 2003). The determination in laboratory of both FC and WP based on arbitrary pressure heads using a pressure plate apparatus may be adequate for some applications, but it ignores the dynamic nature of the involved processes. In fact, no simple and accurate method exists for either field or laboratory determinations of soil water storage (Bhattacharya, 2019; Bittelli, 2009; de Jong van Lier et al., 2019; Silva et al., 2014; Tolk, 2003).

The drought stress expressed as a function of the fraction p of TAW is a rough simplification of soil-vegetation-atmosphere transfer processes, as recognized by Allen et al. (1998). The proper prediction of the LP should consider soil hydraulic properties (retention and conductivity), root density distribution over depth, and atmospheric water demand (de Willigen et al., 2012; dos Santos et al., 2017). The latter factor is only implicitly considered by the widely used FAO method. Similar considerations are valid regarding WP (van den Berg and Driessen, 2002), while for the upper limit of PAW, the FC concept remains ambiguous and subject to criticism (Assouline and Or, 2014; Turek et al., 2022).

The correct determination of upper and lower limits of TAW and RAW is important, and mismatches may lead to inaccuracies in practical applications of TAW and RAW, like in predictions from bucket-type hydrological models, or in irrigation scheduling and management. In this context, the assumption of non-stressed cropping conditions or a "well-watered crop" (Allen et al., 2021; Pereira et al., 2020) required to determine the crop coefficient (k_c), which is a globally accepted approach for computation of crop water requirements (Pereira et al., 2015), cannot be sustained if the limits of plant available water are not adequately addressed.

A process-based determination of upper and lower limits of PAW would allow improving the versatility of TAW and RAW prediction. Recently, Inforsato and de Jong van Lier (2021) developed polynomial functions to predict flux-based FC water content, Θ_{FC} from soil hydraulic parameters. They defined FC as a soil property related to an average profile water content, hence to a soil water storage, considering a predefined depth and drainage rate. For stand-alone use, the polynomials allow the prediction of Θ_{FC} for monolayer soils with known parameters of the Van Genuchten – Mualem (VGM) soil hydraulic functions (Van Genuchten, 1980). Regarding the LP, de Jong Van Lier et al. (2006) proposed an implicit numerical root water uptake model based on matric flux potential (M) to estimate the average soil water content at the onset of crop drought stress (Θ_{LP}). Later, de Jong van Lier et al. (2009) derived an analytic expression for $M(\Theta)$ for VGM type soils, and Pinheiro et al. (2018) derived an expression to calculate M at LP independently of soil depth. Based on these proposals, it is possible to calculate flux-based FC and flux-based LP considering soil hydraulic properties and depth, rooting characteristics, and atmospheric conditions.

In this study, we present a new method to predict PAW based on flux-based approaches for FC and LP (de Jong Van Lier et al., 2006; Inforsato and de Jong van Lier, 2021; Pinheiro et al., 2018), and a novel flux-based approach for WP, composing the flux-based method (FBM). Using this framework, we aim to predict PAW in Van Genuchten – Mualem type soils for different FC flux criteria, soil depths, root densities, and potential transpiration rates, quantify the variability of FC, LP, WP, RAW, and TAW explained by each parameter of the FBM, compare some predictions of the FBM with those of the traditional FAO method, and apply the FBM in both sink-limited and source-limited experimental conditions for plant transpiration.

2. Material and methods

2.1. Theory

2.1.1. Field capacity

Field capacity (FC) is a soil physical quantity related to soil water dynamics, originally defined by Veihmeyer and Hendrickson (1931). It refers to a profile water status corresponding to an arbitrarily established "negligible" drainage rate and can be assessed by means of an internal drainage experiment, in situ or simulated, without evapotranspiration, and starting at saturation in field conditions. A flux-based approach to calculate the water content and pressure head at FC (respectively θ_{FC} and h_{FC}) based on numerical simulations is the full polynomial expression derived by Inforsato and De Jong van Lier (2021). The FC predictors are the negligible flux criterion q_{FC}, the soil depth Z, and the soil hydraulic properties (retention and conductivity) expressed by the Van Genuchten – Mualem (VGM) hydraulic function parameters (Van Genuchten, 1980):

$$\Theta = \frac{\theta - \theta_r}{\theta_s - \theta_r} = \left[1 + (\alpha|h|)^n\right]^{\frac{1}{n}-1} \tag{1}$$

$$K = K_s \Theta^l \left[1 - \left(1 - \Theta^{\frac{n}{n-1}}\right)^{\frac{n-1}{n}}\right]^2 \tag{2}$$

where Θ is the effective saturation, θ ($m^3\ m^{-3}$) is the volumetric soil water content, θ_r ($m^3\ m^{-3}$) and θ_s ($m^3\ m^{-3}$) are the residual and saturated soil water content, respectively, K ($m\ d^{-1}$) is the soil hydraulic conductivity, K_s ($m\ d^{-1}$) is the saturated hydraulic conductivity, and α (m^{-1}), n and l are model fitting parameters.

2.2. Limiting point

The limiting point (LP) defines the onset of the falling rate phase of crop transpiration (de Jong Van Lier et al., 2006; Metselaar and de Jong van Lier, 2007). Defining the matric flux potential M as the integral of the hydraulic conductivity function [$K(h)$]

$$M = \int_{h_{ref}}^{h} K dh \tag{3}$$

where h_{ref} (m) is the lowest allowable root surface pressure head, and under non-hysteretic conditions, M is uniquely correlated to θ and h (M-

θ-*h*).

Based on the theory developed by de Jong van Lier et al. (2006), Pinheiro et al. (2018) showed that for a soil with *k* layers, each with a thickness L_i (m) and a root length density R_i (m^{-2}), the matric flux potential at the onset of transpiration limiting hydraulic conditions (viz.: drought stress), M_{LP} ($m^2\ d^{-1}$), can be predicted by

$$M_{LP} = \frac{pT_p}{\sum_{i=1}^{k} L_i R_i} \quad (4)$$

where T_p (m d^{-1}) is the potential transpiration rate and p is a constant equal to $5.3/\pi = 1.69$. For a monolayer soil of depth Z, Eq. (4) reduces to

$$M_{LP} = \frac{1.69T_p}{ZR} \quad (5)$$

Note that the value of M_{LP} is independent of soil type, whereas its respective pressure head h_{LP} and the soil water content θ_{LP} – corresponding to the onset of limiting soil hydraulic conditions, at M_{LP} – are dependent on the soil hydraulic properties. Using the VGM hydraulic functions (Van Genuchten, 1980), M can be related to h and θ (de Jong van Lier et al., 2009), and h_{LP} and θ_{LP} can be determined for each soil. At water contents higher than θ_{LP}, no drought stress occurs, and transpiration is sink–limited (determined by atmospheric conditions). Below θ_{LP}, transpiration becomes source–limited (restricted by soil conditions).

2.3. Wilting point

The permanent wilting point (WP) commonly refers to the soil water content at a pressure head of –150 m. Simply relating WP to a specific soil water energy implies considering it independent of plant species and soil texture (Liu et al., 2022; Minasny and McBratney, 2018; Wiecheteck et al., 2020). However, as for the limiting point, experimental research showed that both pressure head and water content at WP are not a unique value for a specific soil, but are also dependent on crop characteristics and atmospheric conditions (Angus and van Herwaarden, 2001; Cabelguenne and Debaeke, 1998; Hsieh et al., 1972; Rawlins et al., 1968; Wiecheteck et al., 2020).

The value of h and θ at the soil-root interface when the LP and the WP occur has been of mathematical interest for dynamic root water uptake (RWU) models (Couvreur et al., 2012; de Jong van Lier et al., 2013, 2008; de Willigen and van Noordwijk, 1987; Gardner, 1960; Hillel et al., 1975; Javaux et al., 2013, 2008; Moldrup et al., 1992; Philip, 1957). In these models, the RWU rate is dependent on the soil water diffusivity, the root radius, the root length density, the rooting depth, and the plant transpiration rate.

Based on such models and on the experimental findings of Sinclair and Ludlow (1986), and Sinclair et al. (2005), we hypothesize that as the soil dries below θ_{LP} (the onset of drought stress and source-limited transpiration), stomata closure will proceed, and canopy water vapor conductance will decrease until reaching a minimum value slightly greater than zero resulting from imperfect stomata closure and/or cuticular transpiration. It corresponds to a residual transpiration rate equal to $T_p f_{WP}$, where f_{WP} is the ratio between the minimum and the maximum (potential) canopy water vapor conductance. The water content corresponding to this residual transpiration rate is the wilting point, θ_{WP}. Any further drying of the soil below θ_{WP} will lead to a root water uptake lower than the residual transpiration, and if this condition persists for more than a tolerable time, it will lead to permanent wilting and crop failure.

Consequently, and analogous to Eq. (5), the matric flux potential at wilting point, M_{WP} ($m^2\ d^{-1}$), as well as the associated h_{WP} and θ_{WP} can be predicted by

$$M_{WP} = \frac{1.69T_p f_{WP}}{ZR} = M_{LP} f_{WP} \quad (6)$$

2.4. Implementation of the theory

The flowchart in Fig. 1 shows the implementation of the FC-polynomial, M_{LP} (Eq. (5)), and M_{WP} (Eq. (6)) approaches to predict, respectively, flux-based θ_{FC}, θ_{LP}, and θ_{WP}. To calculate θ_{FC}, the full FC-polynomial expression developed by Inforsato and de Jong van Lier (2021) was applied using the Van Genuchten – Mualem hydraulic parameters, the soil depth Z, and the FC flux criterion q_{FC} as predictors. The resulting effective saturation at field capacity (Θ_{FC}) was then expressed as the soil water content at field capacity θ_{FC} using the suitable Van Genuchten – Mualem function (Fig. 1).

To find θ_{LP}, we first calculated M_{LP} as in Eq. (5), using the soil or rooting depth Z, the root length density R, and the potential transpiration T_p as predictors. Then, θ_{LP} was obtained using an inverse solution for the $M(\theta)$ expressions derived by de Jong van Lier et al. (2009), and h_{LP} was calculated from θ_{LP} using the Van Genuchten – Mualem analytical functions. To calculate θ_{WP}, an analogous procedure was applied (Eq. (6)), in which an additional parameter – the wilting factor f_{WP} – is required to calculate the M_{WP}, and consequently, θ_{WP} (Fig. 1). Finally, RAW and TAW were calculated making RAW = $\theta_{FC} - \theta_{LP}$, and TAW = $\theta_{FC} - \theta_{WP}$.

As a courtesy to the reader, a software to apply this framework was programmed in FORTRAN (F90) and is available on https://github.com/marinalamelo/flux_based_PAW. The input parameters required to run the software are: Z (m), R (cm cm^{-3}), T_p (mm d^{-1}), q_{FC} (mm d^{-1}), f_{WP}, K_s (m d^{-1}), θ_s, θ_r, α (m^{-1}), n, and l (Fig. 1). This software was used to assess the predictions of PAW in three simulated scenarios and two observed scenarios described in the next sections.

2.5. Simulated scenarios

Three general scenarios were simulated to assess the predictions of FC, LP, WP, TAW, and RAW according to the proposed flux-based method (FBM): i) a standard scenario of generic soil-plant-atmosphere conditions, from which sensitivity analyses were performed; ii) a scenario of a specific crop on several soils to compare the predictions of the FBM with those of the FAO method; iii) a scenario of mean plant-atmosphere conditions to map PAW from soil texture using the FBM and the FAO method. The procedures to parametrize each general simulated scenario will be presented in the following.

i) Standard scenario

A standard scenario of a homogeneously rooted soil profile was

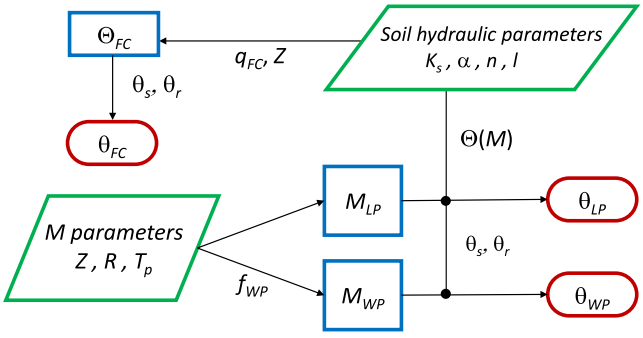

Fig. 1. Flowchart of the flux–based calculation of water content at field capacity θ_{FC}, at limiting point θ_{LP}, and at wilting point θ_{WP}. Θ_{FC} is calculated as a function of the Van Genuchten-Mualem soil hydraulic parameters, the FC flux criterion q_{FC}, and the soil depth Z. M_{LP} is calculated as a function of the soil or rooting depth Z, the root length density R and the potential transpiration T_p. M_{WP} is calculated as M_{LP} but using an additional parameter, the wilting factor f_{WP}. The considered soil hydraulic parameters refer to the Van Genuchten – Mualem hydraulic functions.

parameterized. Values of soil or rooting depth, root length density, potential transpiration, and FC flux criterion were defined for a generic annual crop (Table 1). For the VGM soil hydraulic parameters, average values for the silt loam textural class of the USDA textural triangle were used (Carsel and Parrish, 1988). For the wilting factor (f_{WP}), an approximation was made using average values of maximum canopy conductance and minimum leaf conductance for cereal crops presented in literature reviews (Duursma et al., 2019; Waring and Running, 2007). Data of minimum conductance were converted from mol m^{-2} s^{-1} to m s^{-1} using equation 8.12 in Pearcy et al. (2000) assuming isothermal conditions, an atmospheric pressure of 101.3 kPa, and a leaf temperature of 25 °C. The soil water content and the pressure head associated with FC, LP, and WP, and the corresponding PAW, were predicted according to our flux-based theory following the procedure illustrated in Fig. 1.

From the standard scenario, a sensitivity analysis was performed to quantify the variability of FC, LP, WP, RAW and TAW explained by each parameter (Z, R, T_p, K_s, α, n, l, q_{FC}, and f_{WP}). As we introduced the concept of a residual transpiration rate equal to $T_p{\cdot}f_{WP}$ associated with the wilting point, some complementary analyses were performed to quantify the variability of TAW explained by the wilting factor f_{WP}, and the effect of f_{WP} on the sensitivity of TAW to other parameters.

ii) PAW for a specific crop

The proposed FBM to predict PAW was compared with the traditional FAO method applied to a maize crop, for several soils. The soils were represented by average hydraulic parameters (K_s, θ_r, θ_s, α, and n) estimated by Carsel and Parrish (1988) for the 12 texture classes of the USDA Soil Texture Classification (Table 2). The continuity-tortuosity parameter l was set to its standard value of 0.5 for all soils.

For the FAO method, the water content at FC and the WP was associated with pressure heads of –1 m and –150 m, respectively. The water content at the LP was calculated using the depletion fraction p = 0.55, corresponding to a maize (grain) crop at a 5 mm d^{-1} evapotranspiration rate (ET) (Allen et al., 1998). For the flux-based method, PAW was predicted considering rooting depth Z equivalent to the effective rooting depth of the FAO method, which was set 1 m according to Table 22 in Allen et al. (1998), and potential transpiration T_p equal to ET (5 mm d^{-1}), i.e., negligible soil evaporation. The FC flux criterion (q_{FC}) and the wilting factor (f_{WP}) were set 1 mm d^{-1} and 10^{-2}, respectively. Since root data are often unavailable, and to evaluate the sensitivity of estimations, the flux-based PAW was predicted for three scenarios of root length density R (0.01, 0.1, and 1.0 cm cm^{-3}), i.e., for a low, medium, and high R scenario.

iii) Mapping PAW from soil texture

The prediction of PAW by the FBM relies on information about the soil hydraulic properties (Fig. 1), which is often unavailable.

Table 1
Parameters for a standard scenario of a homogeneously rooted soil profile with hydraulic properties for a silt loam soil (Van Genuchten – Mualem function).

	Symbol	Value	Unit
Soil or rooting depth	Z	0.5	m
Root length density	R	0.5	cm cm^{-3}
Potential transpiration	T_p	4	mm d^{-1}
FC flux criterion	q_{FC}	1	mm d^{-1}
Saturated hydraulic conductivity	K_s	0.11	m d^{-1}
VGM parameters	θ_r	0.067	m m^{-3}
	θ_s	0.450	m m^{-3}
	α	2.0	m^{-1}
	n	1.41	
	l	0.5	
Wilting factor	f_{WP}	10^{-2}	

Table 2
Hydraulic parameters according to the Van Genuchten – Mualem function for the 12 texture classes of the USDA Soil Texture Classification (Carsel and Parrish, 1988). Parameter l was set 0.5 for all soils.

Soil texture type (USDA Soil Texture Classification)	Hydraulic parameters				
	K_s	θ_r	θ_s	α	n
	m d^{-1}	m^3 m^{-3}		m^{-1}	
Sand	7.128	0.045	0.43	14.5	2.68
Loamy sand	3.502	0.057	0.41	12.4	2.28
Sandy loam	1.061	0.065	0.41	7.5	1.89
Loam	0.250	0.078	0.43	3.6	1.56
Silt	0.060	0.034	0.46	1.6	1.37
Silt loam	0.108	0.067	0.45	2.0	1.41
Sandy Clay Loam	0.314	0.100	0.39	5.9	1.48
Clay loam	0.062	0.095	0.41	1.9	1.31
Silty clay loam	0.017	0.089	0.43	1.0	1.23
Sandy clay	0.029	0.100	0.38	2.7	1.23
Silty clay	0.005	0.070	0.36	0.5	1.09
Clay	0.048	0.068	0.38	0.8	1.09

Alternatively, the hydraulic parameters can be predicted from pedotransfer functions (PTF), which use more readily available soil properties like particle size distribution, bulk density, and organic matter content (Inforsato and de Jong van Lier, 2021). Here, the well-known PTF Rosetta (Schaap et al., 2001) was used to predict the VGM parameters for both water retention and hydraulic conductivity functions. Rosetta is easily available and is based on an extensive soil database from North America and Europe that continues to be developed. The VGM parameters predicted by Rosetta were used to calculate the water content at FC, LP, and WP, and using these values TAW and RAW were calculated.

Textural triangles were produced representing TAW and RAW using the H2 model of Rosetta, which only requires particle size distribution (sand, silt, and clay contents) as input. The VGM parameters were predicted for all combinations of particle sizes at a 1 % resolution, resulting in 5,151 data points on each triangle. This procedure is analogous to the one performed by Inforsato and de Jong van Lier (2021) to predict Θ_{FC} using their polynomial expression.

The proposed FBM was compared with the FAO method for the 5,151 soil texture combinations with mean plant-atmosphere conditions. For the FAO method, the water content at FC and the WP was associated with a pressure head of –1 m and –150 m, respectively. RAW was calculated as a fraction of TAW using the generic depletion fraction equal to 0.5 (Allen et al., 1998). For the FBM, the soil or rooting depth Z was considered equal to 0.5 m, which is a reasonable value for many crops. The potential transpiration was set 4 mm d^{-1}, the FC flux criterion and the wilting factor were set 1 mm d^{-1} and 10^{-2}, respectively, and three scenarios of root length density (0.01, 0.1, and 1.0 cm cm^{-3}) were considered.

2.6. Observed scenarios

Two field experiments were used to assess the predictions of flux-based FC, LP, WP, TAW, and RAW over time and under contrasting water regimes. The first experiment will be referred to as the fully irrigated (FI) scenario with soybean crop while the second experiment will be referred to as the water deficit (WD) scenario with common bean crop. A description of each experiment will be presented in the following.

2.7. Fully irrigated (FI) scenario

The FI scenario comprises a three ha field in the São Paulo State, southeast Brazil (county of Piracicaba, 22°42′S, 47°38′W, 526 m a.s.l), where soybean (*Glycine* max) was grown between December 2017 and April 2018. The climate is of the Koeppen Cwa type (winter-dry

subtropical with a warm summer). The soil at the experimental plot is a Rhodic Hapludox according to the USDA/Soil Survey Staff classification (USDA, 2014). The soil has a bulk density of 1,489 kg m^{-3} in the A horizon (0–0.2 m) and 1,371 kg m^{-3} in the Bt horizon (0.2–0.6 m). The texture is clayey, with clay contents in the A and Bt horizons of 0.52 and 0.62 kg kg^{-1}, respectively.

Full irrigation was applied from 26 December 2017 to 5 April 2018 using center pivot sprinklers i-Wob® UP3® (Senninger Irrigation, Inc.). The irrigation amounts were scheduled by potential evapotranspiration (ETo) that was determined for both sites with the Priestley-Taylor (PT) method (Priestley and Taylor, 1972) based on solar radiation and air temperature variables that were recorded with sensors that were properly calibrated and with weather data that were checked daily at the on-site weather station. The PT method was applied under minimum advection conditions, using the empirical parameter $\alpha = 1.26$ (Pereira and Villa Nova, 1992). Subsequently, crop evapotranspiration was computed by multiplying ETo by the crop coefficient (Kc) as described in FAO-56 (Allen et al., 1998). The irrigation depth was 378 mm throughout the season, 25 mm on average for each of the 13 applications.

Volumetric soil water content (θ) was measured at two depths (0.2 and 0.5 m) every 30 min, using dielectric probes (METER Group, Inc., model GS3). The GS3 probes use the capacitance method and can measure bulk electrical conductivity and temperature besides water content. For mineral soils, the GS3 accuracy is ± 0.03 m^3 m^{-3} with a resolution of 0.002 m^3 m^{-3} from 0.0–0.4 m^3 m^{-3}, and 0.001 m^3 m^{-3} for > 0.4 m^3 m^{-3}. The sensors were installed in the center of the irrigated area, both in the row and between the rows, at an average depth of 0.20 m (0.18–0.23 m) and 0.50 m (0.48–0.53 m).

Crop evapotranspiration was determined by the surface energy balance using the Bowen ratio (β) method, based on vertical differences in air temperature and vapor pressure (Bowen, 1926). A β system were installed in the center of the field and measured the following weather variables: surface radiation balance (Rn) (Kipp & Zone Inc., model NR-Lite2), soil heat flux (G) (Hukeseflux Inc., model HFP01), measured at two points 0.05 m below the ground, and vertical gradients of air temperature and partial vapor pressure (Vaisala Inc., model HMP155), measured 0.80 m between the sensors and 0.20 m above the canopy. Data were recorded daily at 10-s intervals and stored as 15-min averages by a data-logger (Campbell Scientific, Inc., model CR1000). This experiment was also reported by da Silva et al. (2021) and Marin et al. (2019).

2.8. Water deficit (WD) scenario

The second experiment, referred to here as the water deficit (WD) scenario, was performed in a neighboring field of approximately 990 m^2, where common bean (*Phaseolus vulgaris*) was grown between June and September 2010. The soil is a Rhodic Kanhapludalf according to the USDA/Soil Survey Staff classification (USDA, 2014). The soil has a bulk density of 1,560 kg m^{-3} in the Ap horizon (0–0.2 m) and 1,380 kg m^{-3} in the Bt horizon (0.2–0.8 m). The texture is clayey, with clay contents in the Ap and Bt horizons of 0.58 and 0.68 kg kg^{-1}, respectively.

The experimental area was divided into two plots of 22 m × 22.5 m. A sprinkler irrigation installation was mounted at the site. One plot was irrigated during the whole crop cycle (fully irrigated plot), while the other one was subject to water stress in the reproductive phase (deficit irrigated plot). During the 91 days of field experiment (15 June to 13 September 2010), rainfall was registered on July 13, 14 and 15, with an accumulated depth of 62.9 mm. There were also rain on September 7 (12.8 mm), and September 21 (38 mm), during the ripening period. In total, the fully irrigated plot received 426.5 mm of water and the deficit irrigated plot received 314.5 mm. The deficit irrigated plot was sprinkler irrigated during the initial growing stages until 2 August but subjected to severe water stress after that, in the reproductive phase. To guarantee the survival of the crop, irrigation water were applied three times between August 4 and September 3 (~5 mm), which was defined as the interval of analysis of this study.

Volumetric soil water content (θ) and pressure head (h) were measured at three depths (0.05, 0.15, and 0.30 m) every 30 min, using electrical conductivity sensors (METER Group, Inc., model EC-5) and polymer tensiometers (de Rooij et al., 2009). EC–5 sensors determine θ by measuring the dielectric constant of the media using capacitance/frequency domain principle at a frequency of 70 MHz. For mineral soils, the EC–5 accuracy is ± 0.03 m^3 m^{-3} with a resolution of 0.001 m^3 m^{-3}. The polymer tensiometer is an instrument developed at WUR, The Netherlands, and allows automated measurements of soil water tension throughout the range of interest in environmental studies (h values of –160 m or less, with an accuracy of 0.2 m), far beyond the range covered by conventional tensiometers.

Canopy temperature, used as an indicator of water stress, was also measured every 30 min by an automated infrared thermometer (Apogee Instruments, model SI-111®). Relative transpiration, i.e., the ratio between actual and potential transpiration (T_a/T_p) was calculated from the vapor pressure deficit and canopy temperature between 5 August and 1 September using the Crop Water Stress Index (CWSI) proposed by Idso et al. (1981). T_a/T_p was considered equivalent to 1 – CWSI, as proposed by Jackson et al. (1981). This experiment was also reported by de Jong van Lier et al. (2013), Durigon et al. (2012), and Durigon and de Jong van Lier (2013); more information can be found in their publications.

2.9. Comparison of FBM predictions to experimental data

Daily weather data for Piracicaba were obtained from the University of São Paulo automatic weather station, located on the experimental site of the FI scenario and at a distance of 20 m from the experimental site of the WD scenario. The following daily weather variables are measured by the station: solar radiation (MJ m^{-2} d^{-1}), net radiation (MJ m^{-2} d^{-1}), relative humidity (%), maximum and minimum air temperatures (°C), wind intensity (m s^{-1}), and rainfall (mm).

For the FI scenario (soybean crop), VGM parameters were obtained by fitting simultaneously Eq.1 and Eq. (2) to data of a laboratory evaporation experiment assisted by the Hyprop system (METER Group, Inc.), using undisturbed soil samples collected at three depths (0.05, 0.35 and 0.50 m) with five replicates. For the WD scenario (common bean crop), soil water retention parameters θ_s, θ_r, α, and n were obtained by fitting Eq. (1) to the field measurements of θ and h at the three observation depths. Hydraulic conductivity parameters K_s and l were obtained by fitting Eq. (2) to data of a laboratory evaporation experiment using polymer tensiometers and following the methodology described in Durigon et al. (2011).

To apply the proposed flux-based method to predict plant available water in both observed scenarios (FI and WD), some assumptions were made and they will be reported in the following. Firstly, the period considered included only the reproductive stages of the crops (about 50–80 days after sowing). During this period, both crops were well developed and promoted full soil covering. Therefore, as the application of the method was restricted to a period in which the root parameters may be considered constant and the soil evaporation flux negligible, corresponding assumptions are feasible. In other scenarios, these parameters may have to be provided as time series over the crop growing period, as is commonly done for potential transpiration.

Soil or rooting depth Z was considered equal to 0.5 m for both FI and WD scenarios, which is a reasonable value for typical soybean and common bean crops in Brazil (da Silva et al., 2021; Durigon et al., 2012). Root length density R was set 0.2 cm cm^{-3} for the FI scenario (soybean), and 0.5 cm cm^{-3} for the WD scenario (common bean), according to de Willigen and van Noordwijk (1987). For field capacity, a flux-based estimate (Inforsato and de Jong van Lier, 2021) was used corresponding to a profile depth of 0.5 m and a bottom flow q_{FC} of 1 mm d^{-1} for both scenarios.

The water flux at the depth of 0.5 m was determined for both

scenarios by simulation of internal drainage experiments performed with the SWAP model v. 4.0.1 (Kroes et al., 2017). To do so, the saturated hydraulic conductivity and VGM parameters obtained at different depths were used to parametrize the soil hydraulic properties, described in SWAP by the parameters θ_r, θ_s, α, n, K_s and l of the VGM functions, Eqs. (1) and (2). Then, to derive a unique set of parameters for each soil profile, the parameter estimation algorithm PEST (Doherty, 2016) was linked with SWAP. The PEST algorithm minimized the differences between the water flux obtained in the simulated drainage experiments using the fitted VGM parameters for the FI and WD scenarios and the water flux simulated for the same scenarios with a unique set of parameters for each soil profile. The obtained optimized root mean squared error of prediction was 0.0071 cm d^{-1} for the FI scenario, and 0.0001 cm d^{-1} for the WD scenario. These procedures of parameter estimation were necessary because the FBM relies on the assumption of homogeneous soil hydraulic conditions over the soil profile.

Potential transpiration T_p was set equal to potential or crop evapotranspiration (ET_c) over the period of time evaluated. For the soybean crop (FI scenario), T_p was set equal to ET_c obtained from the Bowen ratio method. For the common bean crop (WD scenario), T_p was set equal to ET_c calculated from daily weather data using the Penman-Monteith equation and the crop coefficient at the mid-season stage (Allen et al. 1998). For both scenarios, the wilting factor was set at 10^{-2} following Pinheiro et al. (2019). A summary of the parameter values used to describe the FI and WD scenarios is presented in Table 3 except for T_p, which varied with daily weather conditions.

3. Results and discussion

3.1. PAW assessed by the flux-based method

The proposed flux-based method to predict plant available water (PAW) provided reasonable values for the soil water content (θ) and the pressure head (h) at field capacity (FC), at limiting point (LP), at wilting point (WP), and consequently for the readily available water (RAW) and the total available water (TAW) for the simulated standard soil-plant-atmosphere scenario (Table 4). θ_{FC} was 0.10 m^3 m^{-3} lower than the saturated soil water content (Table 1), θ_{LP} was 0.185 m^3 m^{-3} lower than θ_{FC}, and θ_{WP} was 0.056 m^3 m^{-3} lower than θ_{LP} (Table 4). The associated pressure heads (h_{FC}, h_{LP}, and h_{WP}) were within the reported ranges of observed values in the literature (Cassel and Nielsen, 1986; Durigon et al., 2012; Silva et al., 2014; Wiecheteck et al., 2020). RAW represented 76 % of TAW, which is higher than the depletion fraction for almost all crops given in Allen et al. (1998), even for relatively drought-tolerant plants like conifer trees. It suggests that the FBM may predict higher values of RAW compared to the FAO method. This suggestion will be evaluated in the next sections.

Table 3
Parameters used to describe two observed scenarios in Piracicaba, Brazil, with contrasting water regimes: fully irrigated (FI) secnario with soybean crop and water deficit (WD) secnario with common bean crop.

	Symbol	Value		Unit
		FI	WD	
Soil or rooting depth	Z	0.5	0.5	m
Root length density	R	0.2	0.5	cm cm^{-3}
FC flux criterion	q_{FC}	1	1	mm d^{-1}
Saturated hydraulic conductivity	K_s	0.174	0.001	m d^{-1}
VGM parameters	θ_r	0.284	0.075	m m^{-3}
	θ_s	0.448	0.364	m m^{-3}
	α	4.095	0.058	m^{-1}
	n	1.362	1.122	
	l	−1.185	1.146	
Wilting factor	f_{WP}	10^{-2}	10^{-2}	

Table 4
Water content θ and pressure head h at field capacity (FC), at limiting point (LP), at wilting point (WP), and plant available water (RAW and TAW) for a standard scenario of a homogeneously rooted soil profile with hydraulic properties of a silt loam soil, obtained using the flux-based method (FBM).

	Symbol	Value	Unit
Field capacity	θ_{FC}	0.350	m^3 m^{-3}
	h_{FC}	–0.76	m
Limiting point	θ_{LP}	0.165	m^3 m^{-3}
	h_{LP}	–13.77	m
Wilting point	θ_{WP}	0.109	m^3 m^{-3}
	h_{WP}	–112.10	m
Plant available water	RAW	0.185	m^3 m^{-3}
	TAW	0.242	m^3 m^{-3}

3.2. Sensitivity analyses of the flux-based PAW

3.2.1. General analysis

The sensitivity of θ_{FC}, h_{FC}, θ_{LP}, h_{LP}, θ_{WP}, h_{WP}, RAW, and TAW to each parameter of the proposed flux-based PAW (Z, R, T_p, q_{FC}, f_{WP}, K_s, α, n, and l) was assessed considering reasonable ranges of parameter values (Fig. 2, Fig. 3, and Fig. 4). Fig. 2 shows water content and pressure head values as a function of the soil or rooting depth Z, the root length density R, and the potential transpiration T_p. The sensitivity of FC, LP, WP, and TAW to Z was higher for $Z < 0.5$ m (Fig. 2). As both θ_{FC} and θ_{LP} varied similarly with Z, RAW showed a very low sensitivity to Z, varying less than 0.005 m^3 m^{-3} over the entire evaluated range.

R and T_p are not predictors of FC, and therefore show zero sensitivity (Fig. 2). On the other hand, LP, WP, RAW, and TAW were sensitive to R, which indicates that the value of this parameter may require experimental determination. However, it can be less feasible than determining other parameters that the method requires, like T_p, Z, and the soil hydraulic parameters. Root length density R may be one of the most time-intensive parameters to determine, and this may explain the fact that root system quantitative research lags behind the measurements in the much easier accessible aboveground part (Lux and Rost, 2012). A smaller R reduces the plant capacity to extract water from the soil and results in a higher θ_{LP} and θ_{WP}, consequently a lower TAW and RAW. The variation of RAW and TAW over the entire evaluated range of R was 0.168 and 0.062 m^3 m^{-3}, respectively.

The value of T_p had little impact on θ_{WP} and TAW while for θ_{LP}, h_{LP}, h_{WP}, and RAW the impact was considerable but not as significant as for variations in R (Fig. 2). A smaller T_p leads to a lower θ_{LP} and a higher RAW. The small impact of T_p on θ_{WP} and TAW is related to the applied calculation algorithm; note that to obtain M_{WP} (Eq. (5)), T_p is multiplied by the wilting factor f_{WP} (here assumed equal to 0.01). However, a small variation in M may translate into relatively large variations in h, mainly in the drier region of the $M(h)$ curve.

Fig. 3 shows water content and pressure head values as a function of the soil hydraulic parameters (saturated hydraulic conductivity K_s and VGM parameters α, n and l). Sensitivities are mostly not intuitive. The only parameter allowing a simple interpretation is K_s. A smaller K_s leads to higher values of FC, LP, and WP (Fig. 3). This refers to the fact that the values of unsaturated hydraulic conductivity (K) or matric flux potential (M) corresponding to drainage rate (e.g., FC) or root water uptake-related variables (e.g., LP and WP) are reached at a higher water content or pressure head when K_s is lower. Similarly, a higher value of parameter l results in higher gradients of $dK/d\theta$ and $dM/d\theta$, i.e., quicker reduction in conductivity, and critical values of K or M for drainage or water uptake will occur at higher water contents.

The behavior of FC, LP and WP water contents and pressure heads as a function of variations in α and n is less intuitive since they affect both $\theta(h)$ and $K(h)$ without an easy-to-define physical meaning. Both TAW and RAW as functions of α and n present a maximum. For the standard n = 1.41, the maximum TAW occurs at α = 0.89 m^{-1} and the maximum RAW at α = 0.30 m^{-1}. For the standard α = 2.00 m^{-1}, both TAW and

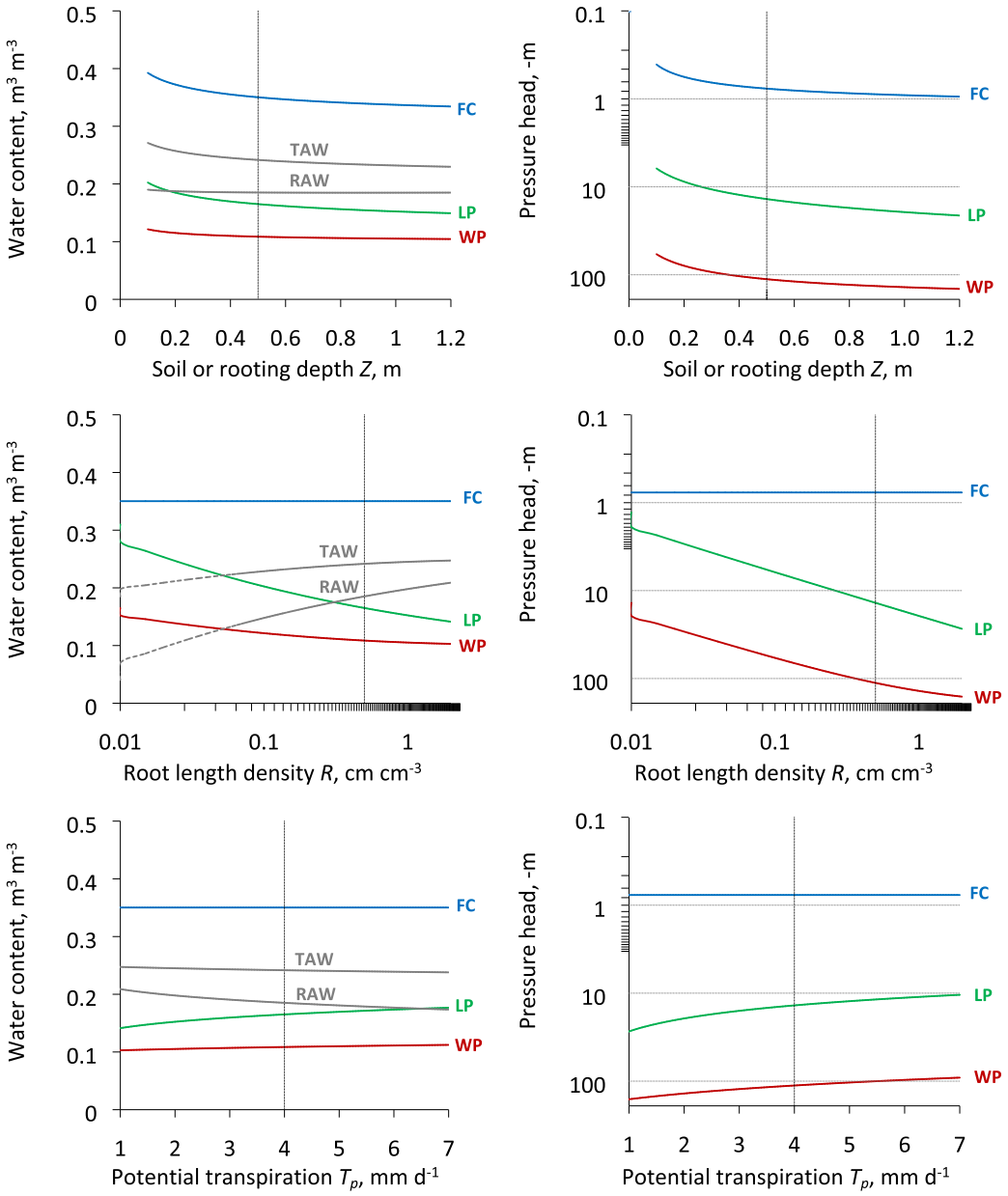

Fig. 2. Water content and pressure head at field capacity (FC), at limiting point (LP), at wilting point (WP), total available water (TAW) and readily available water (RAW) as a function of the soil or rooting depth Z, the root length density R and the potential transpiration T_p, maintaining other parameters at standard values: $Z = 0.5$ m, $R = 0.5$ cm cm^{-3}, $T_p = 4$ mm d^{-1}, $K_s = 0.11$ m d^{-1}, $\alpha = 2.0$ m^{-1}, $n = 1.41$, $l = 0.5$, $q_{FC} = 1$ mm d^{-1}, and $f_{WP} = 10^{-2}$. Vertical lines represent the standard value of the abscissa.

RAW showed a maximum at $n = 1.35$.

Fig. 4 shows water content and pressure head values as a function of the FC flux criterion q_{FC}, and the wilting factor f_{WP}. Only FC is sensitive to q_{FC}, and a smaller q_{FC} leads to a lower FC, hence a lower RAW and TAW, especially for $q_{FC} \leq 1$ mm d^{-1} (Fig. 4). It is important to emphasize that a flux criterion below 1 mm d^{-1} is often unfeasible when it is associated with excessive times to reach FC, frequently in the range between 30 and 60 days (Inforsato and de Jong van Lier, 2021). In the feasible range of q_{FC} between 1 and 4 mm d^{-1}, the maximum variation in both RAW and TAW as a function of q_{FC} was 0.037 m^3 m^{-3}. Thus, the precise definition of q_{FC} seems to be a minor concern compared with the sensitivity to the root and soil hydraulic parameters. However, it should be considered that the impact of q_{FC} on PAW can be different among soil types (Lena et al., 2022). Besides, the impact of q_{FC} on PAW may be major compared to the impact caused by variation in soil organic matter content or other management-induced changes, so proper definition of q_{FC} is important for the application of the method.

The wilting factor f_{WP} only affects WP (Fig. 1). Reducing f_{WP} makes WP correspond to lower water content, hence TAW increases (Fig. 4). The maximum variation in TAW as a function of f_{WP} over the evaluated range from 0.001 to 0.1 was 0.028 m^3 m^{-3}. Thus, the precise definition of f_{WP} also seems to be a minor concern to predict PAW. However, as a novel concept of the WP including the parameter f_{WP} was introduced in our theory, a more detailed assessment regarding f_{WP} will be reported in the next section.

3.2.2. *TAW and the wilting factor*

Besides the standard scenario, the sensitivity of the total available water (TAW) to the wilting factor f_{WP} was assessed for each two other simulated scenarios of rooting depth (Z), root length density (R) and soil

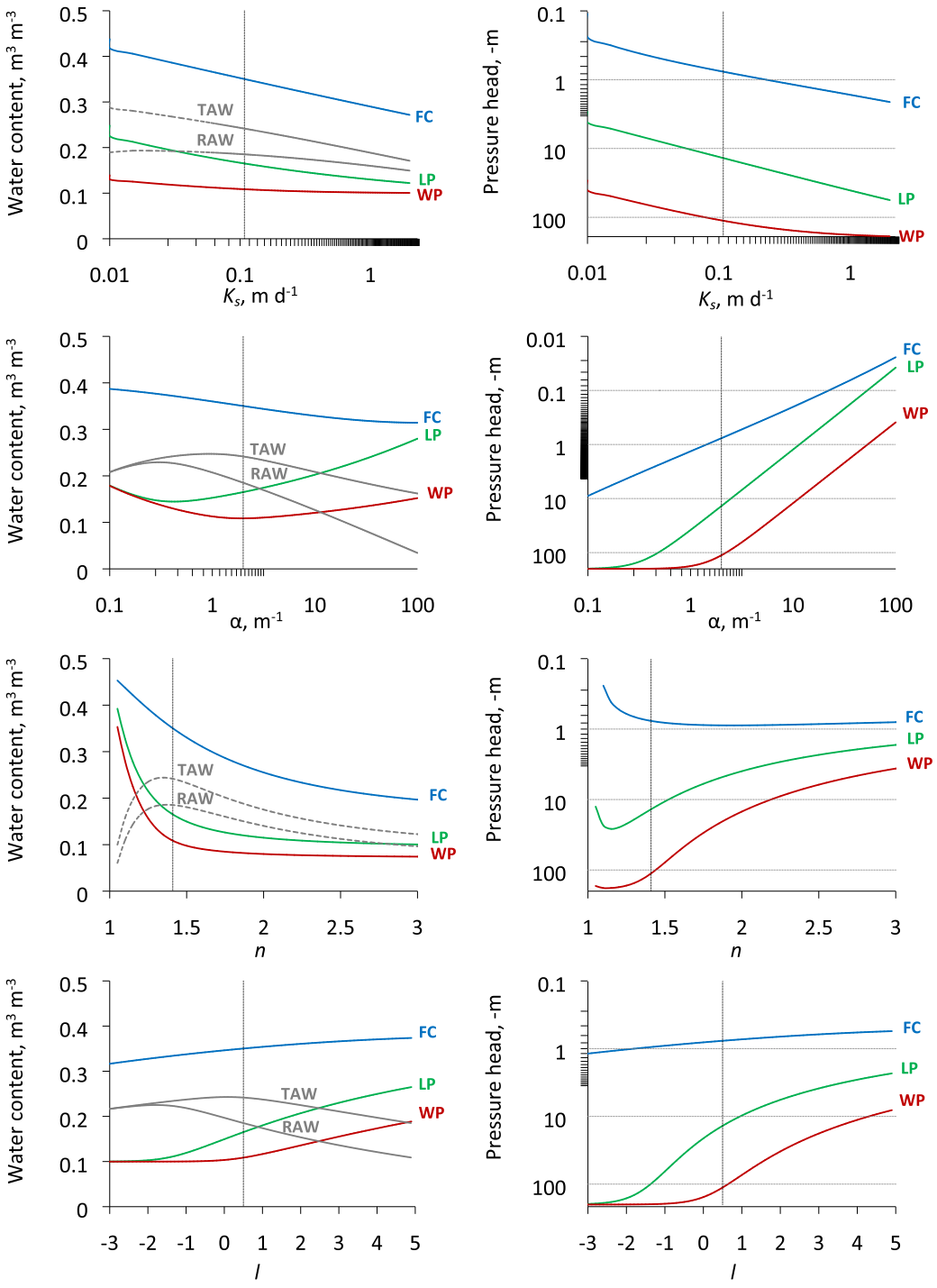

Fig. 3. Water content and pressure head at field capacity (FC), at limiting point (LP), at wilting point (WP), total available water (TAW) and readily available water (RAW) as a function of the saturated hydraulic conductivity K_s and the VGM parameters α, n and l, maintaining other parameters at standard values: $Z = 0.5$ m, $R = 0.5$ cm cm^{-3}, $T_p = 4$ mm d^{-1}, $K_s = 0.11$ m d^{-1}, α = 2.0 m^{-1}, $n = 1.41$, $l = 0.5$, $q_{FC} = 1$ mm d^{-1}, and $f_{WP} = 10^{-2}$. Vertical lines represent the standard value of the abscissa.

hydraulic parameters (K_s, α, n, and l). Results are shown in Fig. 5, where the standard scenario is represented by the green lines and indicated with an asterisk.

The sensitivity of TAW to f_{WP} is expected to be higher under conditions where plant drought tolerance is lower, i.e., scenarios with shallow soil depth, low root density, low soil hydraulic conductivity, or quick reduction in conductivity, i.e., high l (Casaroli et al., 2010; Durigon et al., 2012). Fig. 5 confirms this, and simulated scenarios with $Z = 0.1$ m, $R = 0.01$ cm cm^{-3}, $K_s = 0.011$ m d^{-1}, α = 100 m^{-1}, and $l = 3.0$ show higher sensitivities to f_{wp} than scenarios with their standard values. In contrast, for scenarios with higher R, Z, K_S or lower l, the exact value of f_{WP} in the range from 0.001 to 0.1 seems to be of limited importance to predict TAW. Hence, parameter estimation efforts regarding f_{WP} can be driven by the likelihood of plant drought stress.

The value of f_{wp} also affects the sensitivity of TAW to other parameters, mainly to R, α, K_s, and l. A higher value of f_{wp} tends to increase the

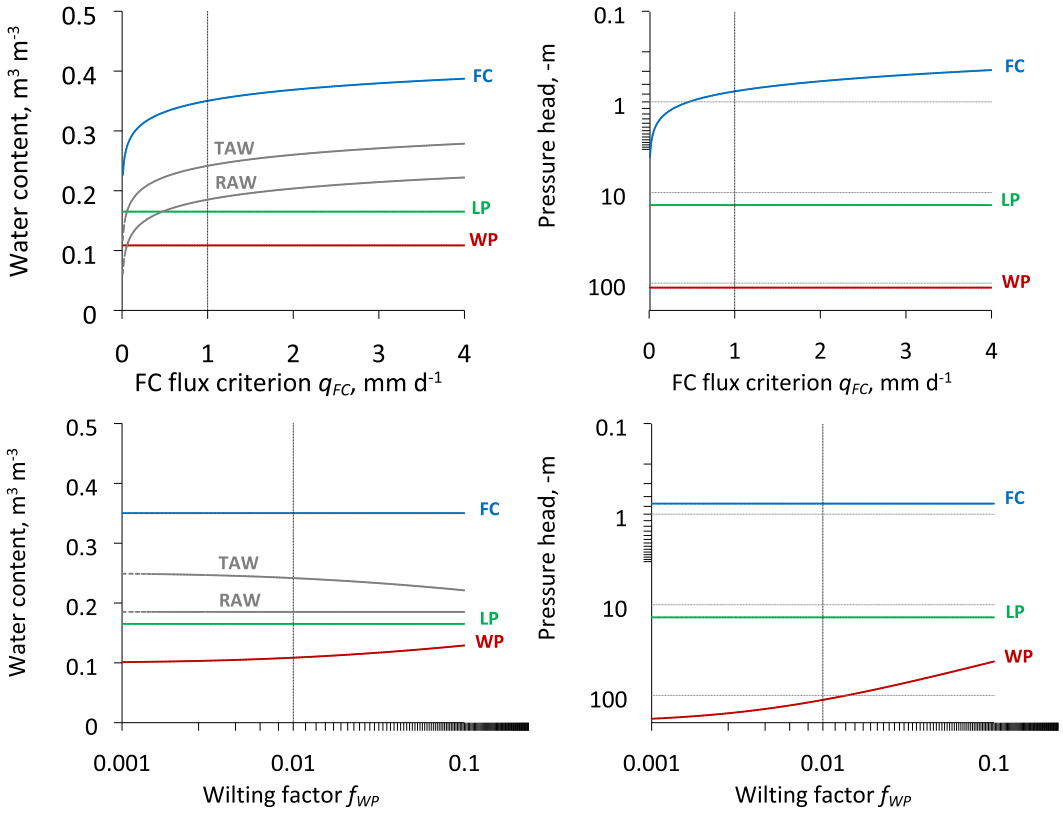

Fig. 4. Water content and pressure head at field capacity (FC), at limiting point (LP), at wilting point (WP), total available water (TAW) and readily available water (RAW) as a function of the field capacity flux criterion q_{FC}, and the wilting factor f_{WP}, maintaining other parameters at standard values: $Z = 0.5$ m, $R = 0.5$ cm cm^{-3}, $T_p = 4$ mm d^{-1}, $K_s = 0.11$ m d^{-1}, $\alpha = 2.0$ m^{-1}, $n = 1.41$, $l = 0.5$, $q_{FC} = 1$ mm d^{-1}, and $f_{WP} = 10^{-2}$. Vertical lines represent the standard value of the abscissa.

sensitivity of TAW to R, α, and l, while it tends to reduce the sensitivity of TAW to K_s (Fig. 6). The combination of low values of R with high values of f_{wp} corresponds to a scenario of few active roots and high residual transpiration, so the plant drought tolerance is low. It corresponds to high water content at wilting point (θ_{WP}) and, consequently, low TAW. In comparison to the standard scenario, the combination of higher values of α or l with higher values of f_{wp} corresponds to scenarios of lower water retention or quicker reduction in conductivity with higher residual transpiration, which reduces TAW. In turn, the combination of higher values of K_s with higher residual transpiration also reduces TAW but the sensitivity is lower because the reduction in θ_{FC} due to higher K_s is greater than the increase in θ_{WP} due to higher f_{wp}, as the general analysis suggests (Fig. 3 and Fig. 4). Based on these analyses, we observed that the proposed method to predict PAW, including a novel flux-based approach to calculate θ_{WP}, reproduces adequately the expected behavior of some soil-plant interactions related to water availability to plants.

3.2.3. An example for a maize crop

The availability of water for a maize crop was predicted according to the FAO method and the proposed FBM for three scenarios of root length density R (high: $R_H = 1$ cm cm^{-3}, medium: $R_M = 0.1$ cm cm^{-3}, and low: $R_L = 0.01$ cm cm^{-3}) in the 12 soil texture classes of the USDA. Using the applied flux criterion $q_{FC} = 1$ mm d^{-1}, the FBM predicts a higher water content at field capacity (θ_{FC}) for all texture classes except for the sandy clay loam (Fig. 7).

In contrast to the FAO method, the FBM enables including factors of root water uptake and transpiration in the prediction of both LP and WP, making it a process-based and more versatile method to predict PAW. This is clear from Fig. 7, which shows that, for the FAO method, RAW is a fixed fraction of TAW ($p = 0.55$) regardless of texture class, i.e., the important interactions between soil hydraulic properties and root water uptake are not considered. On the other hand, the FBM predicts different RAW/TAW ratios depending on the texture class and increasing values for θ_{LP} and θ_{WP} with decreasing R. In this context, in FAO Paper No. 56 (Allen et al., 1998), a correction of the value of the depletion fraction p is suggested for different soil textures, but the procedure is based on empirical and imprecise relations, which may increase the uncertainties in the PAW prediction following the FAO method.

It is interesting to observe that for a few texture classes (sand, loamy sand, and sandy loam) the FBM with the low R (FBM-R_L) predicts a θ_{LP} higher than θ_{FC}. In these cases, θ_{LP} is not shown in the figure, and the crop will experience water stress even at FC. This condition (i.e., when drainage quickly produces a water content limiting transpiration) is physically plausible and may be expected in coarse-textured soils (soils with a high macroporosity and narrow pore-size distribution), in which drainage of water leads to a sharp drop in the pressure head (Pinheiro et al., 2019). For these soil textures, a higher negligible flux criterion may be more suitable to predict FC.

The sensitivity of WP to R was variable among soil texture classes but in most cases, the θ_{WP} values for both methods were similar for the high R. The largest difference between the methods regarding θ_{WP} was observed for the sandy clay loam texture, in which θ_{WP} for the FBM was lower in all R scenarios. For all texture classes, the readily available water (RAW) was higher for the FBM-R_H, and lower for the FBM-R_L in comparison to the FAO method. The total available water (TAW) was similar between the FBM-R_M and the FAO method for eight of the 12 texture classes considered (Fig. 7).

3.3. Soil textural triangle for mapping PAW

The soil texture triangles in Fig. 8 show the prediction of Total

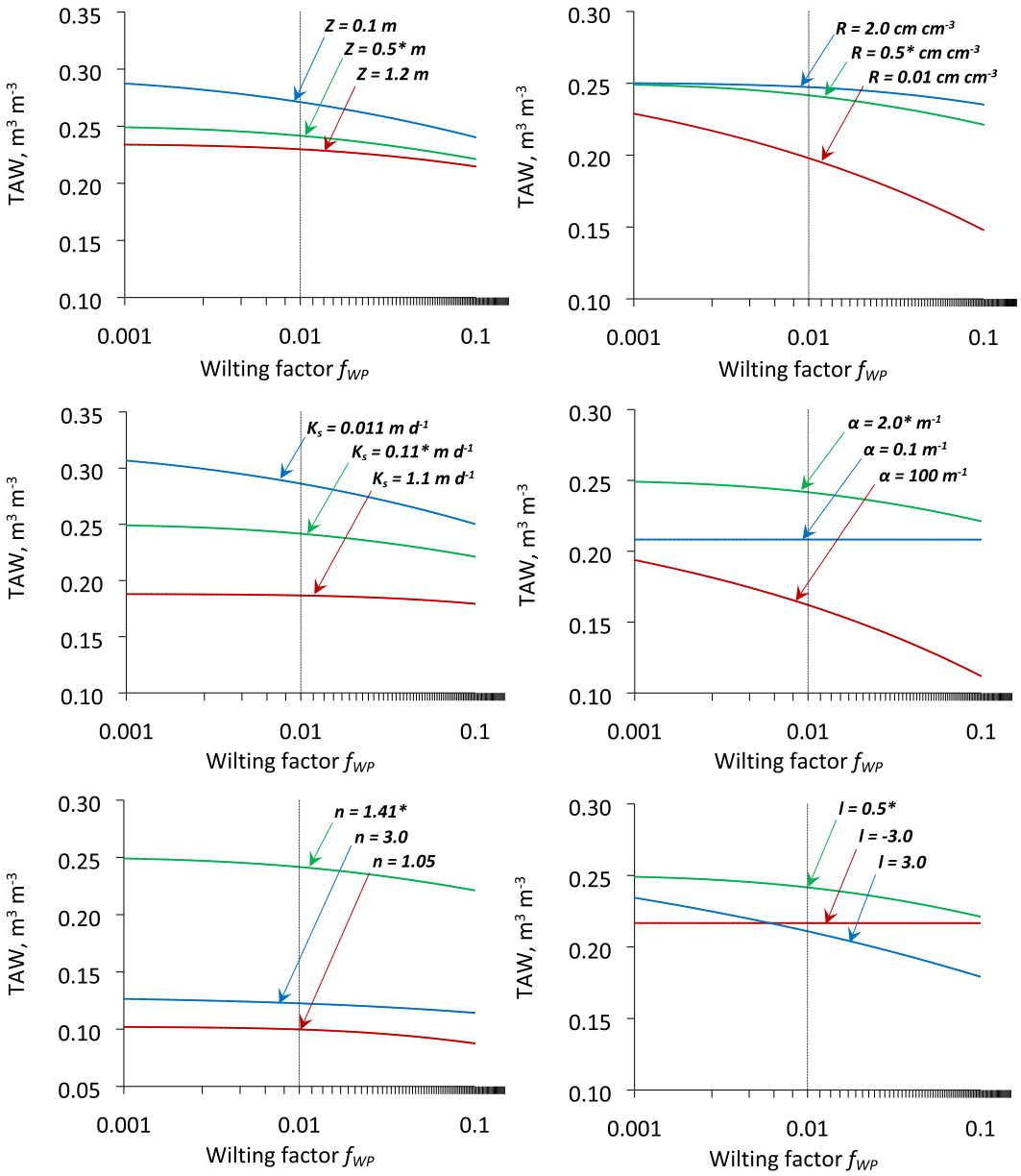

Fig. 5. Total available water (TAW) as a function of wilting factor f_{WP}, for three values of each parameter: soil or rooting depth Z, root length density R, saturated hydraulic conductivity K_s, and VGM parameters α, n, and l, maintaining other parameters at standard values: $Z = 0.5$ m, $R = 0.5$ cm cm^{-3}, $T_p = 4$ mm d^{-1}, $K_s = 0.11$ m d^{-1}, α = 2.0 m^{-1}, $n = 1.41$, $l = 0.5$ and $q_{FC} = 1$ mm d^{-1}. *Standard parameter value. Vertical lines represent the standard value of the wilting factor.

Available Water (TAW) using the Rosetta PTF following the two prediction methods: the FAO method and the proposed flux-based method (FBM). For the FBM, the triangle for the medium root length density $R =$ 0.1 cm cm^{-3} is shown, as not much difference was observed for the low or high R. The FBM provided a more complex behavior of the contour lines related to the soil texture in comparison to the FAO method (Fig. 8). In general, TAW was lower for the FBM (0.026 m^3 m^{-3} lower on average) especially at low sand contents and medium to high silt contents (lower right part of the triangle). The highest difference between the methods occurred at 26 % sand and 74 % silt, for which $TAW_{FBM} - TAW_{FAO}$ was equal to –0.191 m^3 m^{-3}. On the other hand, high sand contents (≥80 % sand) correspond to the lowest TAW values in both methods (Fig. 8).

The FAO method considers fixed arbitrary values of pressure head associated with θ_{FC} and θ_{WP}, independently of the soil hydraulic properties and soil depth. On the other hand, to predict θ_{FC} and θ_{WP} the FBM explicitly considers soil depth and hydraulic properties. Because of these conceptual differences between the methods, the results can be less or more different depending on the scenario, mainly regarding soil hydraulic properties. For example, in Fig. 7 the highest difference in θ_{FC} between the methods was 0.041 m^3 m^{-3} for the sandy clay soil, while in Fig. 8 it was 0.189 m^3 m^{-3} for a silt loam soil (27 % sand and 73 % silt). Note that the results in Fig. 7 were generated from average soil hydraulic parameters values for each texture class (USDA) while the results in Fig. 8 were generated based on Rosetta PTF, which estimates soil hydraulic parameters values for each combination of sand, clay, and silt contents, thus better capturing the sensitivity of PAW to those parameters.

From a more detailed analysis of the silt and silt loam textures in Fig. 8 (lower right part of the triangle, 0–50 % sand and 100–50 % silt), we observed that FBM–θ_{FC} was 0.121 m^3 m^{-3} lower on average than FAO–θ_{FC}, whereas θ_{WP} differed less than 0.001 m^3 m^{-3}. This indicates

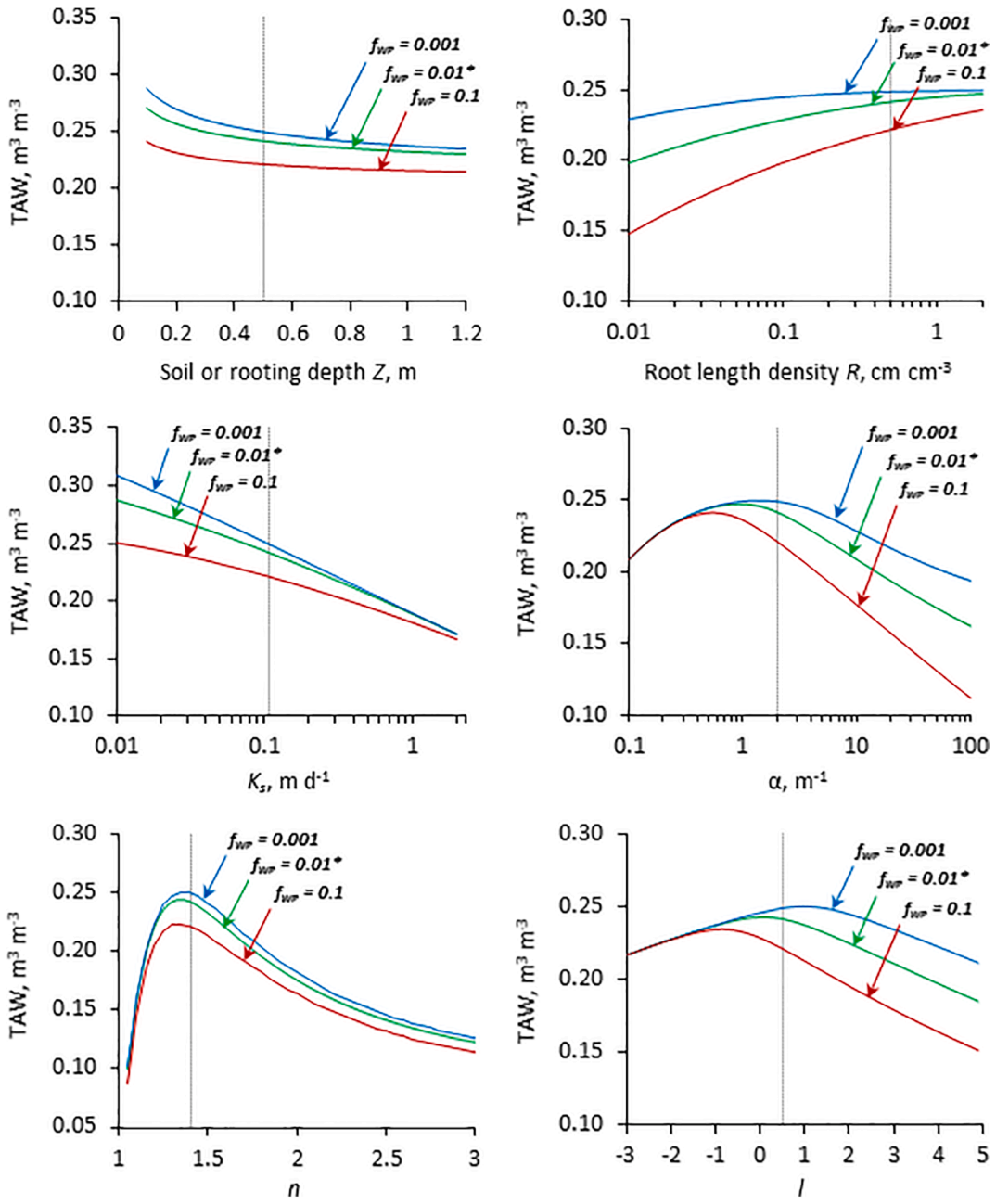

Fig. 6. Total available water (TAW) as a function of soil or rooting depth Z, root length density R, saturated hydraulic conductivity K_s, and VGM parameters α, n, and l, for three values of wilting factor f_{WP}, maintaining other parameters at standard values: $Z = 0.5$ m, $R = 0.5$ cm cm^{-3}, $T_p = 4$ mm d^{-1}, $K_s = 0.11$ m d^{-1}, α = 2.0 m^{-1}, $n = 1.41$, $l = 0.5$ and $q_{FC} = 1$ mm d^{-1}. *Standard parameter value. Vertical lines represent the standard value of the abscissa.

that the differences between FBM and FAO method are mostly due to the distinct values for the upper limit (FC) of TAW rather than for its lower limit (WP). Indeed, this could be expected from the behavior of the soil hydraulic functions and it corroborates the greater interest in FC as a research topic compared to WP (Evett et al., 2019; Reynolds, 2018; Turek et al., 2020).

It is important to emphasize that the pressure head at FC of −1 m widely used in the FAO method and the generic FC flux-criterion of 1 mm d^{-1} used in the FBM are probably not realistic for all particle size distributions, mainly for those less frequently reported in the literature, e.g., very silty soils. Thus, the values of TAW in both triangles of Fig. 8 should not be interpreted as reference values, although they reveal important differences between the methods. In practice, the predictions of the FBM may imply a lower available water capacity for soils with medium to high silt contents (>40 % silt) and a higher available water capacity for soils in the range of 20 %-80 % clay and 0–20 % silt, with implications for the irrigation management.

The soil texture triangles in Fig. 9 show the prediction of Readily Available Water (RAW) for various soil textures according to the FAO method and the FBM, using three values of R for the FBM: 0.01 cm cm^{-3} (low), 0.1 cm cm^{-3} (medium), and 1.0 cm cm^{-3} (high). Unlike TAW-FBM triangles, RAW-FBM triangles showed high sensitivity to R. Similar to results for TAW, the FBM provided less smooth contour lines related to the soil texture in comparison to the FAO method, and the lowest RAW values occurred at the high sand contents (≥80 % sand). The RAW values were generally higher for the FBM; the average difference between the methods (FBM – FAO) was 0.04 m^3 m^{-3} for low R, 0.057 m^3 m^{-3} for medium R, and 0.079 m^3 m^{-3} for high R. The highest difference between the methods was 0.118 m^3 m^{-3} at 36 % sand and 24 % silt, considering the RAW-FBM triangle for high R (Fig. 9).

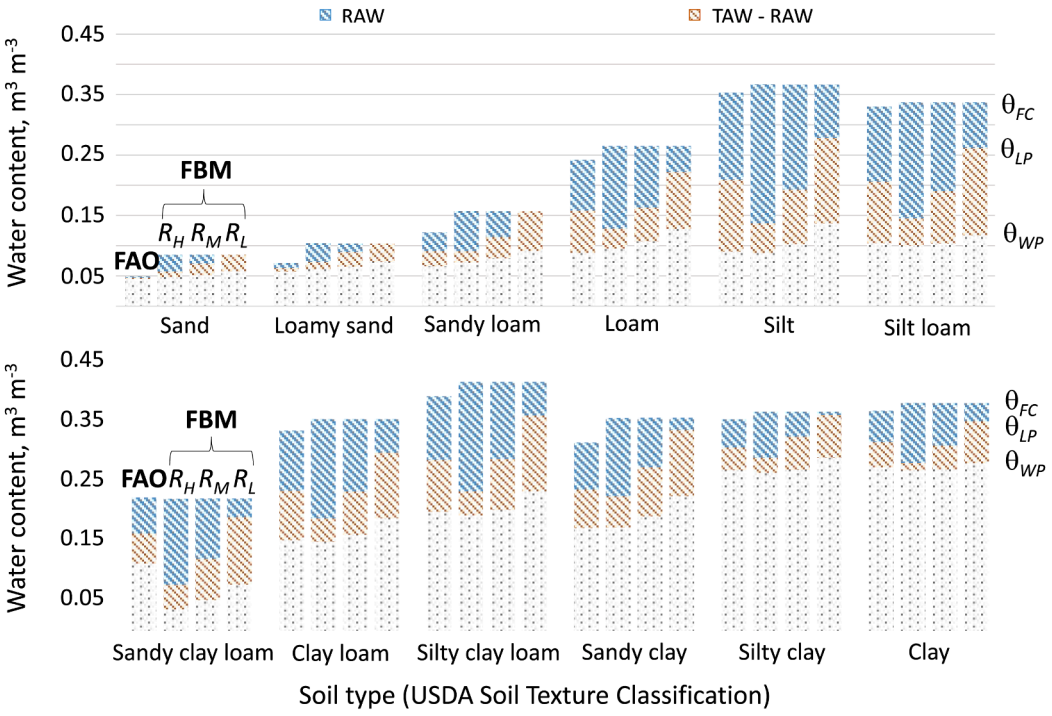

Fig. 7. Readily available water (RAW), total available water (TAW), and water content at field capacity (θ_{FC}), at limiting point (θ_{LP}), and at wilting point (θ_{WP}) estimated according to the FAO method (FAO) and the proposed flux-based method (FBM) for three scenarios of root length density, $R_H = 1$ cm cm^{-3} (high), $R_M = 0.1$ cm cm^{-3} (medium), and $R_L = 0.01$ cm cm^{-3} (low) for maize (grain) in the 12 texture classes of the USA Soil Texture Classification. Fixed parameters: $p = 0.55$, $h_{FC} = -1$ m, $h_{WP} = -150$ m (FAO method); $Z = 1$ m, $q_{FC} = 1$ mm d^{-1}, $f_{WP} = 0.01$, $T_p = 5$ mm d^{-1} (FBM).

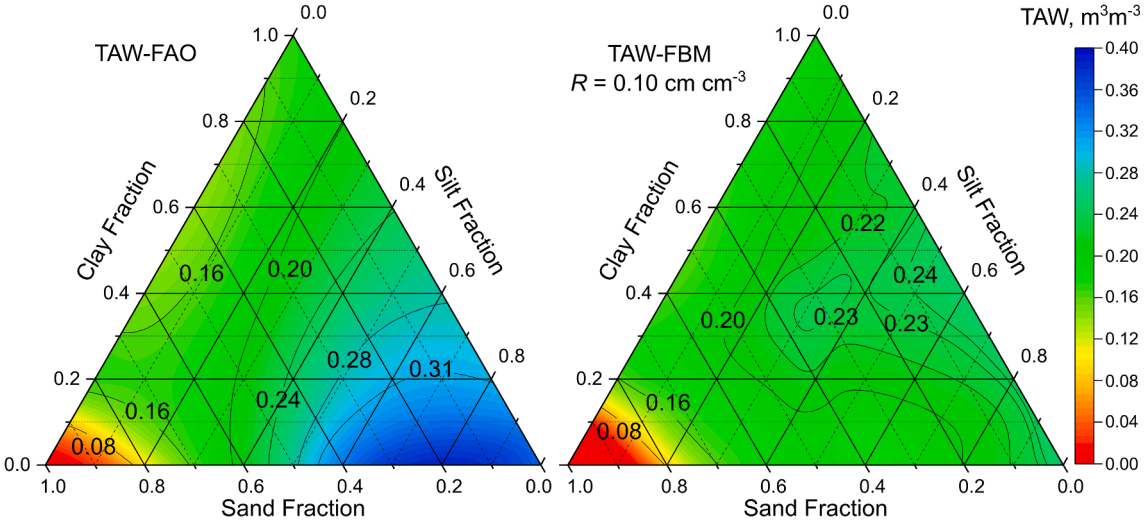

Fig. 8. Soil textural triangles of total available water (TAW) predicted by the FAO method (left) and the proposed flux-based method (FBM, right), using the VGM soil hydraulic parameters estimated by Rosetta for each combination of sand, clay, and silt contents. Fixed parameters: $p = 0.5$, $h_{FC} = -1$ m, $h_{WP} = -150$ m (FAO method); $Z = 0.5$ m, $q_{FC} = 1$ mm d^{-1}, $f_{WP} = 0.01$, $T_p = 4$ mm d^{-1}, and $R = 0.1$ cm cm^{-3} (FBM).

The higher RAW values predicted by the FBM were mostly due to its prediction of a lower θ_{LP} (0.108 m^3 m^{-3} lower on average for high R). This result corresponds to the fact that the FBM tends to predict higher values of RAW compared to the FAO method, mainly for medium to high R, as suggested in Fig. 7. Since the FAO method does not consider the effect of root length density on PAW, it may underestimate RAW for scenarios with dense root systems, e.g. grass and agroforestry buffers (Kumar et al., 2010). Hence, the improved prediction of PAW by the FBM, which considers the effect of rooting characteristics on PAW, would allow optimizing irrigation management and raising water productivity for any rooting condition as long as it is well parametrized.

3.4. Flux-based PAW in contrasting water regimes

The predictions of the proposed flux-based method for PAW were assessed for two observed scenarios of annual crops in the municipality of Piracicaba, Brazil (geographical coordinates 22.704° S and 47.634° W), under contrasting water regimes (Figs. 10 and 11). Unlike the simulated scenarios, these observed scenarios allow evaluating the application of the FBM for time series of water demand and supply and,

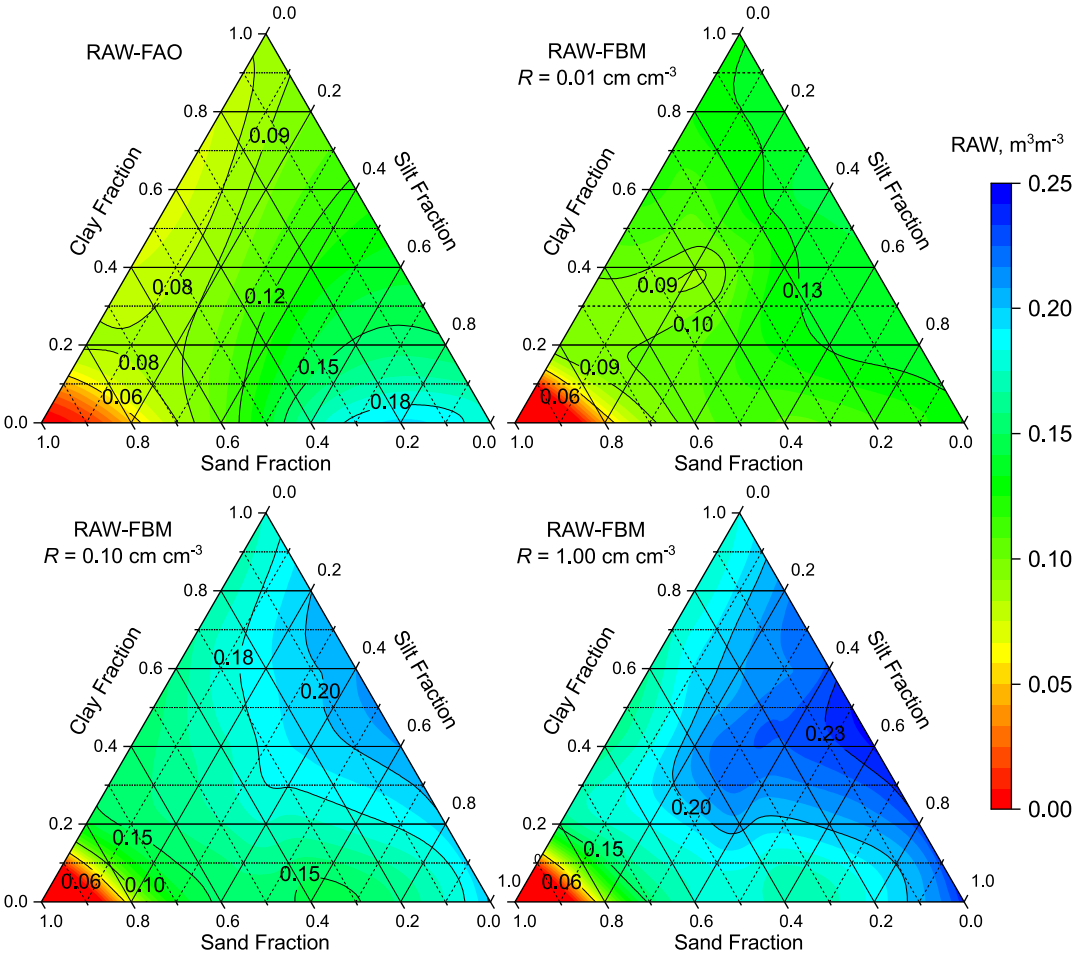

Fig. 9. Soil textural triangle of readily available water (RAW) predicted by the FAO method (top, right) and the proposed flux-based method (FBM) for three values of root length density R: R = 0.01 cm cm^{-3}, R = 0.1 cm cm^{-3}, and R = 1.0 cm cm^{-3}, using the VGM soil hydraulic parameters estimated by Rosetta for each combination of sand, clay, and silt contents. Fixed parameters: p = 0.5, h_{FC} = –1 m, h_{WP} = –150 m (FAO method); Z = 0.5 m, q_{FC} = 1 mm d^{-1}, f_{WP} = 0.01, and T_p = 4 mm d^{-1} (FBM).

therefore, closer to its practical use.

In the first scenario, which comprises a fully irrigated (FI) soybean crop, soil water content (WC) was expected to stay close to field capacity (FC), and above the limiting point (LP) and the wilting point (WP) since there was no water deficit, i.e., the crop water requirements were fully supplied. Indeed, the predicted values for the LP and the WP were always below the observed WC values at the depths of 0.2 m and 0.5 m during 50–80 days after planting (DAP). The predicted values were 0.089 m^3 m^{-3} and 0.107 m^3 m^{-3} lower on average for the LP and the WP, respectively, considering the two depths measured. Additionally, the observed WC values at the depth of 0.2 m were close to the value predicted for FC on 18 of the 31 days considered (Fig. 10). Therefore, the FBM predicted RAW values corresponding to the no drought-stress condition and sink-limited transpiration assumed in the experimental design. TAW and RAW values predicted in the evaluated period were in the range of 0.09–0.10 m^3 m^{-3} and 0.07–0.09 m^3 m^{-3}, respectively (Fig. 10).

In the second and contrasting scenario, comprising a common bean crop under water deficit (WD), WC was expected to fall below FC, and stay below the LP and/or close to the WP in at least part of the rooted zone, since the crop was exposed to drought stress conditions during the evaluated period (50–80 DAP). The observed values of relative transpiration, i.e., the ratio between actual and potential transpiration (T_a/T_p) obtained from canopy temperature measurements, fell below 0.5 on 60 DAP and reached values close to zero on 79 DAP (Fig. 11).

For this scenario, the observed WC values at the depth of 0.05 m were always below the predicted WP for the soil profile (0.114 m^3 m^{-3} below the WP on average). These low water contents in the surface layer can be explained by the fact that roots preferentially extracted water from this layer during the first weeks when water contents were high, leading to the very low values after 50 DAP. Note that the predicted WP refers to the effective hydraulic properties of the entire rooting depth (section 2.5), so water contents in a specific layer can drop below the predicted WP by root water uptake. In contrast, at the depth of 0.30 m, the observed WC values were always above the WP, the LP and even the FC (0.086 m^3 m^{-3} above the LP on average). To survive under these conditions, roots adjust to near-surface drought by extracting water from deeper and wetter layers (Lai and Katul, 2000).

At the intermediate depth (0.15 m), the observed WC values were below the predicted values for the LP from 63 DAP to 80 DAP (0.012 m^3 m^{-3} below the LP on average), i.e., the FBM could predict water deficit at this depth for the major part of the evaluated period. Furthermore, the observed WC values were slightly below the predicted values for the WP from 66 DAP to 80 DAP (0.006 m^3 m^{-3} below the WP on average), with a slight recovery on 79 DAP because of irrigation (Fig. 11). Based on these results for the WD scenario, it can be considered that the FBM was able to predict drought stress in at least part of the rooted zone, and transpiration was predominantly source-limited. TAW and RAW values predicted in the evaluated period were around 0.042 m^3 m^{-3} and 0.035 m^3 m^{-3}, respectively (Fig. 11).

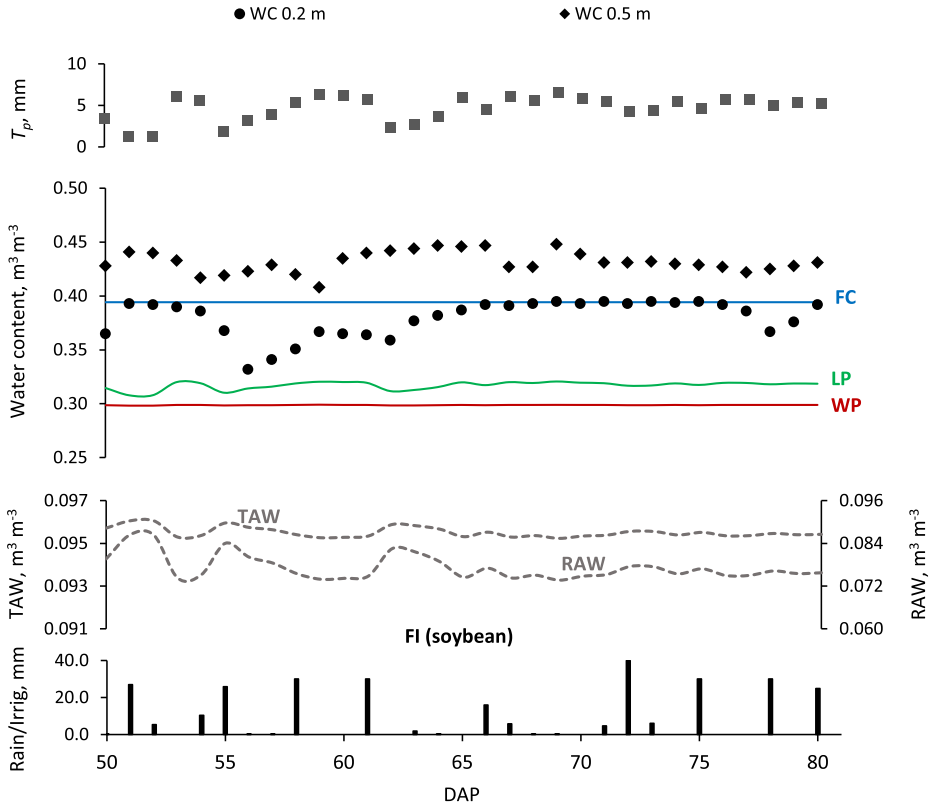

Fig. 10. Observed potential transpiration (T_p), soil water content (WC) at depths of 0.2 m and 0.5 m, and rain or irrigation (Rain/Irrig.), together with predicted field capacity (FC), limiting point (LP), wilting point (WP), total available water (TAW), and readily available water (RAW) acoording to the proposed flux-based method for the fully irrigated (FI) scenario with soybean during 50–80 days after planting (DAP) in Piracicaba, Brazil.

Even with the simplifications and assumptions made to assess the proposed FBM for PAW in two observed scenarios, the predictions of the method were plausible with observed data of soil water content in both sink-limited and source-limited conditions for plant transpiration. This outcome reveals the potential of the FBM to improve irrigation management strategies, avoid productivity losses due to water stress and even allow the saving of irrigation water. Although theoretically sound, the FBM needs to be intensively tested in numerous observed scenarios or field experiments to better evaluate its performance in comparison to the FAO method, an objective that requires broad environmental prospecting and may be addressed in the future.

Our method allows predicting PAW in VGM type soils for different FC flux criteria, soil depths, potential transpiration rates, and root densities. Since free drainage conditions are assumed at the bottom of the soil profile, the influence of groundwater levels and capillary rise on FC is neglected. The ability of plants to use water between saturation and FC (de Jong van Lier, 2017) is also neglected since FC is assumed as the upper limit of PAW. Despite these limitations, the proposed flux-based method is an advance in the process-based prediction of PAW, which may help overcome some limitations of the traditional calculation of PAW.

Further development of this method should address the flux-criterion for FC as the upper limit of PAW, the bottom boundary condition for shallow groundwater tables, as well as a comprehensive evaluation on the residual transpiration rate that defines the permanent wilting point. Other studies are encouraged to address the accuracy of the FBM using experimental data of soil water content related to plant water status, water uptake or transpiration rates, and even crop productivity in different environmental conditions. The FBM can also be compared with other methods to predict and map PAW for different soil textures, like those presented by Al Majou et al. (2008), Ferreira (2017), McNeill et al. (2018), and Ramos et al. (2014). Based on the outcomes of this study, we evaluate that the FBM is a promising approach to predict PAW mediated by unsaturated soil water flow, rooting characteristics, and atmospheric water demand, serving an important role in vadose zone research.

4. Conclusion

A flux-based method (FBM) to predict plant available water (PAW) was introduced. The FBM does not make use of any traditional pressure head value to define field capacity (FC) and the wilting point (WP), nor does it apply empirical parameters to calculate the limiting point (LP). After applying the FBM to several scenarios, we conclude that:

1. Root length density (R) and soil hydraulic parameters (K_s, and VGM α, n, l) explain most of the variability of FC, LP, WP, RAW, and TAW predicted according to the FBM.
2. For maize crop scenarios, the FBM tended to predict higher water contents at FC than the FAO method, while the WP can be similar to the common practice of adopting a fixed pressure head of –150 m, as in the FAO method, mainly in high to medium R scenarios.
3. Texture triangles of TAW are little affected by R, and the differences between the FBM and FAO method are mostly due to the distinct values for FC. Texture triangles of RAW are strongly affected by R, and the differences between the FBM and FAO method are mostly due to the distinct values for the LP.
4. The predictions of the FBM agreed with observed data of soil water content in soybean and common bean field experiments in southeastern Brazil under dynamic conditions of sink-limited and source-limited transpiration.
5. The calculation of PAW by the FBM for scenarios of different soil, plant, and atmosphere conditions may help improving irrigation management strategies, resulting in savings of irrigation water.

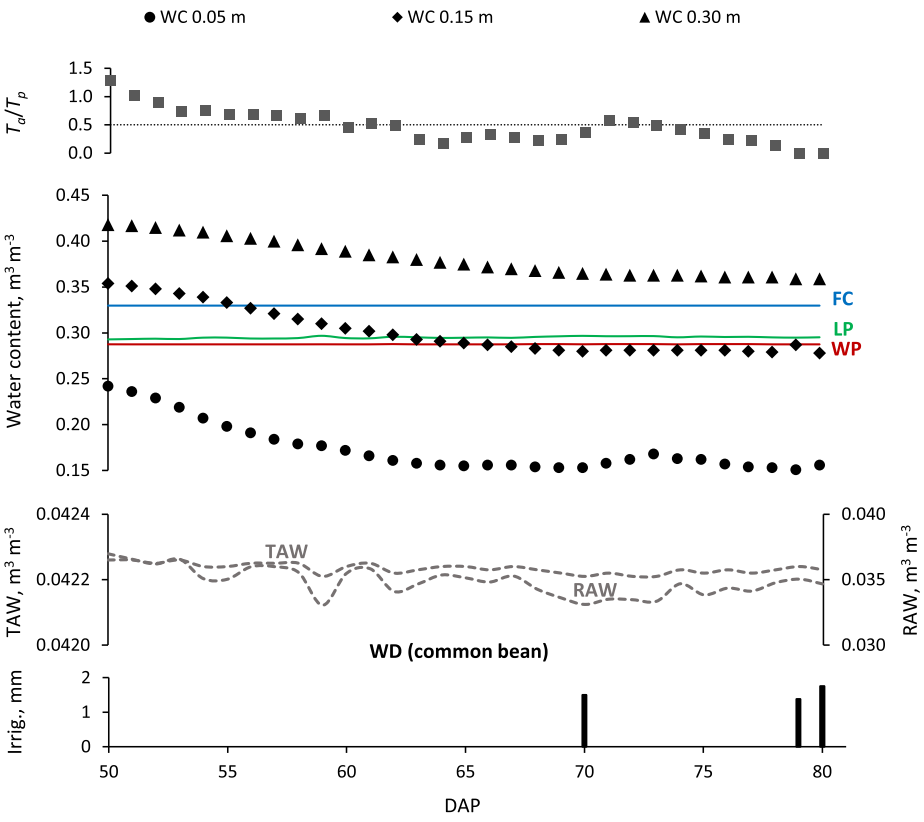

Fig. 11. Observed relative transpiration (T_a/T_p), soil water content (WC) at depths of 0.05 m, 0.15 m and 0.30 m, and irrigation (Irrig.), together with predicted field capacity (FC), limiting point (LP), wilting point (WP), total available water (TAW), and readily available water (RAW) acoording to the proposed flux-based method for the water defict (WD) scenario with common bean during 50–80 days after planting (DAP) in Piracicaba, Brazil.

Declaration of Competing Interest

The authors declare that they have no known competing financial interests or personal relationships that could have appeared to influence the work reported in this paper.

Data availability

Data will be made available on request.

Funding

The research leading to this publication was supported by the National Council for Scientific and Technological Development (CNPq, Brazil), grant number 141197/2020–0, and the São Paulo Research Foundation (FAPESP, Brazil), grant numbers 2022/00853-2, 2020/07294–3, 2020/00145–2, and 2018/20902–2.

References

Al Majou, H., Bruand, A., Duval, O., Le Bas, C., Vautier, A., 2008. Prediction of soil water retention properties after stratification by combining texture, bulk density and the type of horizon. Soil Use Manag. 24, 383–391. https://doi.org/10.1111/j.1475-2743.2008.00180.x.

Allen, R.G., Kilic, A., Robison, C.W., 2021. Current Frameworks for Reference ET and Crop Coefficient Calculation. Presented at the 6th Decennial National Irrigation Symposium, 6-8, December 2021, San Diego, California, ASABE, St. Joseph, MI, p. 1. 10.13031/irrig.2020-070.

Allen, R.G., Pereira, L.S., Raes, D., Smith, M., 1998. Crop evapotranspiration-Guidelines for computing crop water requirements-FAO Irrigation and drainage paper 56. Rome Food Agric. Organ. U. N. 56, e156.

Angus, J.F., van Herwaarden, A.F., 2001. Increasing Water Use and Water Use Efficiency in Dryland Wheat. Agron. J. 93, 290–298. https://doi.org/10.2134/agronj2001.932290x.

Assouline, S., Or, D., 2014. The concept of field capacity revisited: Defining intrinsic static and dynamic criteria for soil internal drainage dynamics. Water Resour. Res. 50, 4787–4802. https://doi.org/10.1002/2014WR015475.

Bhattacharya, A., 2019. Chapter 3 - Water-Use Efficiency Under Changing Climatic Conditions, in: Bhattacharya, A. (Ed.), Changing Climate and Resource Use Efficiency in Plants. Academic Press, pp. 111–180. 10.1016/B978-0-12-816209-5.00003-9.

Bittelli, M., 2009. Errors in Water Retention Curves Determined with Pressure Plates. Soil Sci. Soc. Am. J. 73, 1453–1460. https://doi.org/10.2136/sssaj2008.0082.

Bowen, I.S., 1926. The ratio of heat losses by conduction and by evaporation from any water surface. Phys. Rev. 27, 779.

Cabelguenne, M., Debaeke, P., 1998. Experimental determination and modelling of the soil water extraction capacities of crops of maize, sunflower, soya bean, sorghum and wheat. Plant Soil 202, 175–192. https://doi.org/10.1023/A:1004376728978.

Carsel, R.F., Parrish, R.S., 1988. Developing joint probability distributions of soil water retention characteristics. Water Resour. Res. 24, 755–769. https://doi.org/10.1029/WR024i005p00755.

Casaroli, D., van Lier, Q. de J., Neto, D.D., 2010. Validation of a root water uptake model to estimate transpiration constraints. Agric. Water Manag. 97, 1382–1388. https://doi.org/10.1016/j.agwat.2010.04.004.

Cassel, D.K., Nielsen, D.R., 1986. Field Capacity and Available Water Capacity. In: Methods of Soil Analysis. John Wiley & Sons Ltd, pp. 901–926. https://doi.org/10.2136/sssabookser5.1.2ed.c36.

Couvreur, V., Vanderborght, J., Javaux, M., 2012. A simple three-dimensional macroscopic root water uptake model based on the hydraulic architecture approach. Hydrol. Earth Syst. Sci. 16, 2957–2971. https://doi.org/10.5194/hess-16-2957-2012.

da Silva, E.H.F.M., Boote, K.J., Hoogenboom, G., Gonçalves, A.O., Junior, A.S.A., Marin, F.R., 2021. Performance of the CSM-CROPGRO-soybean in simulating soybean growth and development and the soil water balance for a tropical environment. Agric. Water Manag. 252, 106929 https://doi.org/10.1016/j.agwat.2021.106929.

de Jong van Lier, Q., 2017. Field capacity, a valid upper limit of crop available water? Agric. Water Manag. 193, 214–220. https://doi.org/10.1016/j.agwat.2017.08.017.

de Jong van Lier, Q., Dourado Neto, D., Metselaar, K., 2009. Modeling of transpiration reduction in van Genuchten-Mualem type soils. Water Resour. Res. 45 https://doi.org/10.1029/2008WR006938.

de Jong van Lier, Q., Logsdon, S., Pinheiro, E., Gubiani, P., 2022. Plant available water. 10.1016/B978-0-12-822974-3.00043-4.

de Jong Van Lier, Q., Metselaar, K., Van Dam, J.C., 2006. Root water extraction and limiting soil hydraulic conditions estimated by numerical simulation. Vadose Zone J. 5, 1264–1277. https://doi.org/10.2136/vzj2006.0056.
de Jong van Lier, Q., Pinheiro, E.A.R., Inforsato, L., 2019. Hydrostatic Equilibrium between Soil Samples and Pressure Plates Used in Soil Water Retention Determination: Consequences of a Questionable Assumption. Rev. Bras. Ciênc. Solo. https://doi.org/10.1590/18069657rbcs20190014.
de Jong van Lier, Q., Van Dam, J., Metselaar, K., De Jong, R., Duijnisveld, W., 2008. Macroscopic root water uptake distribution using a matric flux potential approach. Vadose Zone J. 7, 1065–1078. https://doi.org/10.2136/vzj2007.0083.
de Jong van Lier, Q., Wendroth, O., 2016. Reexamination of the Field Capacity Concept in a Brazilian Oxisol. Soil Sci. Soc. Am. J. 80, 264–274. https://doi.org/10.2136/sssaj2015.01.0035.
de Jong van Lier, Q., van Dam, J.C., Durigon, A., Dos Santos, M.A., Metselaar, K., 2013. Modeling water potentials and flows in the soil–plant system comparing hydraulic resistances and transpiration reduction functions. Vadose Zone J. 12 https://doi.org/10.2136/vzj2013.02.0039.
de Rooij, G.H., van der Ploeg, M.J., Gooren, H.P.A., Bakker, G., Hoogendam, C.W., Huiskens, C., Kruidhof, H., Koopal, L.K., 2009. Measuring very negative water potentials with polymer tensiometers: principles, performance and applications. Biologia (Bratisl.) 64, 438–442. https://doi.org/10.2478/s11756-009-0077-8.
de Willigen, P., van Noordwijk, M., 1987. Roots, plant production and nutrient use efficiency. Wageningen University and Research.
de Willigen, P., van Dam, J.C., Javaux, M., Heinen, M., 2012. Root water uptake as simulated by three soil water flow models. Vadose Zone J. 11 https://doi.org/10.2136/vzj2012.0018.
Doherty, J., 2016. PEST model-independent parameter estimation user manual part I: PEST, SENSAN and Global Optimisers. Watermark Numer. Comput. 6.
dos Santos, M.A., de Jong van Lier, Q., van Dam, J.C., Freire Bezerra, A.H., 2017. Benchmarking test of empirical root water uptake models. Hydrol. Earth Syst. Sci. 21, 473–493. https://doi.org/10.5194/hess-21-473-2017.
Durigon, A., Alex dos Santos, M., de Jong van Lier, Q., Metselaar, K., 2012. Pressure heads and simulated water uptake patterns for a severely stressed bean crop. Vadose Zone J. 11 https://doi.org/10.2136/vzj2011.0187.
Durigon, A., de Jong van Lier, Q., 2013. Canopy temperature versus soil water pressure head for the prediction of crop water stress. Agric. Water Manag. 127, 1–6. https://doi.org/10.1016/j.agwat.2013.05.014.
Durigon, A., Gooren, H.P.A., van Lier, Q.D., Metselaar, K., 2011. Measuring Hydraulic Conductivity to Wilting Point Using Polymer Tensiometers in an Evaporation Experiment. Vadose Zone J. 10, 741–746. https://doi.org/10.2136/vzj2010.0057.
Duursma, R.A., Blackman, C.J., Lopéz, R., Martin-StPaul, N.K., Cochard, H., Medlyn, B. E., 2019. On the minimum leaf conductance: its role in models of plant water use, and ecological and environmental controls. New Phytol. 221, 693–705. https://doi.org/10.1111/nph.15395.
Evett, S.R., Stone, K.C., Schwartz, R.C., O'Shaughnessy, S.A., Colaizzi, P.D., Anderson, S. K., Anderson, D.J., 2019. Resolving discrepancies between laboratory-determined field capacity values and field water content observations: implications for irrigation management. Irrig. Sci. 37, 751–759. https://doi.org/10.1007/s00271-019-00644-4.
Ferreira, M.I., 2017. Stress Coefficients for Soil Water Balance Combined with Water Stress Indicators for Irrigation Scheduling of Woody Crops. Horticulturae 3, 38. https://doi.org/10.3390/horticulturae3020038.
Gardner, W.R., 1960. Dynamic aspects of water availability to plants. Soil Sci. 89.
Hillel, D., Beek, V., Talpaz, H., 1975. A microscopic-scale model of soil water uptake and salt movement to plant roots. Soil Sci. 120, 385–399.
Hsieh, J.J.C., Gardner, W.H., Campbell, G.S., 1972. Experimental Control of Soil Water Content in the Vicinity of Root Hairs. Soil Sci. Soc. Am. J. 36, 418–421. https://doi.org/10.2136/sssaj1972.03615995003600030017x.
Idso, S.B., Jackson, R.D., Pinter, P.J., Reginato, R.J., Hatfield, J.L., 1981. Normalizing the stress-degree-day parameter for environmental variability. Agric. Meteorol. 24, 45–55. https://doi.org/10.1016/0002-1571(81)90032-7.
Inforsato, L., de Jong van Lier, Q., 2021. Polynomial functions to predict flux-based field capacity from soil hydraulic parameters. Geoderma 404. https://doi.org/10.1016/j.geoderma.2021.115308.
Jackson, R., Idso, S., Reginato, R., Pinter, P., 1981. Canopy temperature as a crop water stress indicator. https://doi.org/10.1029/WR017I004P01133.
Javaux, M., Schröder, T., Vanderborght, J., Vereecken, H., 2008. Use of a three-dimensional detailed modeling approach for predicting root water uptake. Vadose Zone J. 7, 1079–1088. https://doi.org/10.2136/vzj2007.0115.
Javaux, M., Couvreur, V., Vanderborght, J., Vereecken, H., 2013. Root water uptake: From three-dimensional biophysical processes to macroscopic modeling approaches. Vadose Zone J. 12 https://doi.org/10.2136/vzj2013.02.0042.
Kirkham, M.B., 2005. 8 - Field Capacity, Wilting Point, Available Water, and the Non-Limiting Water Range. In: Kirkham, M.B. (Ed.), Principles of Soil and Plant Water Relations. Academic Press, Burlington, pp. 101–115. https://doi.org/10.1016/B978-012409751-3/50008-6.
Kristensen, J.A., Balstrøm, T., Jones, R.J.A., Jones, A., Montanarella, L., Panagos, P., Breuning-Madsen, H., 2019. Development of a harmonised soil profile analytical database for Europe: a resource for supporting regional soil management. SOIL 5, 289–301. https://doi.org/10.5194/soil-5-289-2019.
Kroes, J.G., Dam, J.C. van, Bartholomeus, R.P., Groenendijk, P., Heinen, M., Hendriks, R. F.A., Mulder, H.M., Supit, I., Walsum, P.E.V. van, 2017. SWAP version 4. https://doi.org/10.18174/416321.
Kumar, S., Udawatta, R.P., Anderson, S.H., 2010. Root length density and carbon content of agroforestry and grass buffers under grazed pasture systems in a Hapludalf. Agrofor. Syst. 80, 85–96. https://doi.org/10.1007/s10457-010-9312-0.
Lai, C.-T., Katul, G., 2000. The dynamic role of root-water uptake in coupling potential to actual transpiration. Adv. Water Resour. 23, 427–439. https://doi.org/10.1016/S0309-1708(99)00023-8.
Lena, B.P., Bondesan, L., Pinheiro, E.A.R., Ortiz, B.V., Morata, G.T., Kumar, H., 2022. Determination of irrigation scheduling thresholds based on HYDRUS-1D simulations of field capacity for multilayered agronomic soils in Alabama, USA. Agric. Water Manag. 259, 107234 https://doi.org/10.1016/j.agwat.2021.107234.
Liu, H., Rezanezhad, F., Lennartz, B., 2022. Impact of land management on available water capacity and water storage of peatlands. Geoderma 406, 115521. https://doi.org/10.1016/j.geoderma.2021.115521.
Logsdon, S., 2019. Should Upper Limit of Available Water be Based on Field Capacity? Agrosystems Geosci. Environ. 2, 190066 https://doi.org/10.2134/age2019.08.0066.
Lux, A., Rost, T.L., 2012. Plant root research: the past, the present and the future. Ann. Bot. 110, 201–204. https://doi.org/10.1093/aob/mcs156.
Luz, F., Castioni, G., Tormena, C., Freitas, R., Carvalho, J., Cherubin, M., 2022. Soil tillage and machinery traffic influence soil water availability and air fluxes in sugarcane fields. Soil Tillage Res. 223, 105459 https://doi.org/10.1016/j.still.2022.105459.
Marin, F.R., Angelocci, L.R., Nassif, D.S.P., Vianna, M.S., Pilau, F.G., da Silva, E.H.F.M., Sobenko, L.R., Gonçalves, A.O., Pereira, R.A.A., Carvalho, K.S., 2019. Revisiting the crop coefficient-reference evapotranspiration procedure for improving irrigation management. Theor. Appl. Climatol. 138, 1785–1793. https://doi.org/10.1007/s00704-019-02940-7.
McNeill, S.J., Lilburne, L.R., Carrick, S., Webb, T.H., Cuthill, T., 2018. Pedotransfer functions for the soil water characteristics of New Zealand soils using S-map information. Geoderma 326, 96–110. https://doi.org/10.1016/j.geoderma.2018.04.011.
Metselaar, K., de Jong van Lier, Q., 2007. The shape of the transpiration reduction function under plant water stress. Vadose Zone J. 6, 124–139. https://doi.org/10.2136/vzj2006.0086.
Minasny, B., McBratney, A.B., 2018. Limited effect of organic matter on soil available water capacity. Eur. J. Soil Sci. 69, 39–47. https://doi.org/10.1111/ejss.12475.
Moldrup, P., Rolston, D., Hansen, J.A., Yamaguchi, T., 1992. A simple, mechanistic model for soil resistance to plant water uptake. Soil Sci. 153, 87–93. https://doi.org/10.1097/00010694-199202000-00001.
Pearcy, R.W., Schulze, E.-D., Zimmermann, R., 2000. Measurement of transpiration and leaf conductance, in: Pearcy, R.W., Ehleringer, J.R., Mooney, H.A., Rundel, P.W. (Eds.), Plant Physiological Ecology: Field Methods and Instrumentation. Springer Netherlands, Dordrecht, pp. 137–160. 10.1007/978-94-010-9013-1_8.
Pereira, L.S., Allen, R.G., Smith, M., Raes, D., 2015. Crop evapotranspiration estimation with FAO56: Past and future. Agric. Water Manag. Priorities Chall. 147, 4–20. https://doi.org/10.1016/j.agwat.2014.07.031.
Pereira, L.S., Paredes, P., Jovanovic, N., 2020. Soil water balance models for determining crop water and irrigation requirements and irrigation scheduling focusing on the FAO56 method and the dual Kc approach. Agric. Water Manag. 241 https://doi.org/10.1016/j.agwat.2020.106357.
Pereira, A.R., Villa Nova, N.A., 1992. Analysis of the Priestley-Taylor parameter. Agric. For. Meteorol. 61, 1–9. https://doi.org/10.1016/0168-1923(92)90021-U.
Philip, J., 1957. The physical principles of soil water movement during the irrigation cycle. Proceedings 3rd Congress International Communications Irrigation Drainage 8: 125–154. 1957.
Pinheiro, E.A.R., de Jong van Lier, Q., Metselaar, K., 2018. A matric flux potential approach to assess plant water availability in two climate zones in Brazil. Vadose Zone J. 17, 1–10. https://doi.org/10.2136/vzj2016.09.0083.
Pinheiro, E.A.R., de Jong van Lier, Q., Inforsato, L., Šimůnek, J., 2019. Measuring full-range soil hydraulic properties for the prediction of crop water availability using gamma-ray attenuation and inverse modeling. Agric. Water Manag. 216, 294–305. https://doi.org/10.1016/j.agwat.2019.01.029.
Priestley, C.H.B., Taylor, R.J., 1972. On the assessment of surface heat flux and evaporation using large-scale parameters. Mon. Weather Rev. 100, 81–92. https://doi.org/10.1175/1520-0493(1972)100<0081:OTAOSH>2.3.CO;2.
Raes, D., Steduto, P., Hsiao, T., Fereres, E., 2018. Chapter 2: Users guide. AquaCrop version 6.0-6.1. Reference Manual. Food Agric. Organ. FAO Rome 2–302.
Ramos, T.B., Horta, A., Gonçalves, M.C., Martins, J.C., Pereira, L.S., 2014. Development of ternary diagrams for estimating water retention properties using geostatistical approaches. Geoderma 230–231, 229–242. https://doi.org/10.1016/j.geoderma.2014.04.017.
Rawlins, S.L., Gardner, W.R., Dalton, F.N., 1968. In Situ Measurement of Soil and Plant Leaf Water Potential. Soil Sci. Soc. Am. J. 32, 468–470. https://doi.org/10.2136/sssaj1968.03615995003200040016x.
Reynolds, W.D., 2018. An analytic description of field capacity and its application in crop production. Geoderma 326, 56–67. https://doi.org/10.1016/j.geoderma.2018.04.007.
Savage, M.J., Ritchie, J.T., Bland, W.L., Dugas, W.A., 1996. Lower Limit of Soil Water Availability. Agron. J. 88, 644–651. https://doi.org/10.2134/agronj1996.00021962008800040024x.
Schaap, M.G., Leij, F.J., van Genuchten, M.T., 2001. Rosetta: a computer program for estimating soil hydraulic parameters with hierarchical pedotransfer functions. J. Hydrol. 251, 163–176. https://doi.org/10.1016/S0022-1694(01)00466-8.
Silva, B.M., da Silva, É.A., de Oliveira, G.C., Ferreira, M.M., Serafim, M.E., 2014. Plant-available soil water capacity: estimation methods and implications. Rev. Bras. Ciênc. Solo 38, 464–475. https://doi.org/10.1590/S0100-06832014000200011.
Sinclair, T.R., Holbrook, N.M., Zwieniecki, M.A., 2005. Daily transpiration rates of woody species on drying soil. Tree Physiol. 25, 1469–1472. https://doi.org/10.1093/treephys/25.11.1469.

Sinclair, T., Ludlow, M., 1986. Influence of Soil Water Supply on the Plant Water Balance of Four Tropical Grain Legumes. Funct. Plant Biol. 13, 329–341. https://doi.org/10.1071/PP9860329.

Skaggs, T.H., van Genuchten, M.T., Shouse, P.J., Poss, J.A., 2006. Macroscopic approaches to root water uptake as a function of water and salinity stress. Agric. Water Manag. Responsible Management of Water in Agriculture 86, 140–149. https://doi.org/10.1016/j.agwat.2006.06.005.

Tolk, J.A., 2003. Plant available soil water. Encycl. Water Sci. Marcel Dekker Inc N. Y. NY 669–672.

Turek, M.E., de Jong van Lier, Q., Armindo, R.A., 2020. Estimation and mapping of field capacity in Brazilian soils. Geoderma 376, 114557. https://doi.org/10.1016/j.geoderma.2020.114557.

Turek, M.E., Jong, D.e., van Lier, Q., Armindo, R.A., 2022. Parameterizing field capacity as the upper limit of available water in bucket-type hydrological models. Comput. Electron. Agric. 194, 106801 https://doi.org/10.1016/j.compag.2022.106801.

USDA. United States Department of Agriculture, 2014. Keys to Soil Taxonomy. Government Printing Office.

van den Berg, M., Driessen, P.M., 2002. Water uptake in crop growth models for land use systems analysis: I. A review of approaches and their pedigrees. Agric. Ecosyst. Environ. 92, 21–36. https://doi.org/10.1016/S0167-8809(01)00285-7.

Van Genuchten, M.T., 1980. A closed-form equation for predicting the hydraulic conductivity of unsaturated soils. Soil Sci. Soc. Am. J. 44, 892–898. https://doi.org/10.2136/sssaj1980.03615995004400050002x.

Veihmeyer, F., Hendrickson, A., 1931. The moisture equivalent as a measure of the field capacity of soils. Soil Sci. 32, 181–194. https://doi.org/10.1097/00010694-193109000-00003.

Waring, R., Running, S., 2007. CHAPTER 9. The Role of Forests in Global Ecology. https://doi.org/10.1016/B978-012370605-8.50016-5.

Wiecheteck, L.H., Giarola, N.F.B., de Lima, R.P., Tormena, C.A., Torres, L.C., de Paula, A. L., 2020. Comparing the classical permanent wilting point concept of soil (−15,000 hPa) to biological wilting of wheat and barley plants under contrasting soil textures. Agric. Water Manag. 230, 105965 https://doi.org/10.1016/j.agwat.2019.105965.